Selective demolition of masonry unit walls with a soundless chemical demolition agent

Atteyeh S. Natanzi, Ph.D. [a], Debra F. Laefer, Ph.D. [b]*, S.M. Iman Zolanvari, Ph.D. [c]
[a] School of Civil Engineering, University College Dublin, Ireland; atteyeh.natanzi@ucdconnect.ie
[b] Center for Urban Science + Progress, New York University, USA; debra.laefer@nyu.edu
[c] School of Civil Engineering, University College Dublin, Ireland; iman.zolanvari@ucdconnect.ie
Corresponding Author

ABSTRACT

A Soundless Chemical Demolition Agent was applied for selective demolition to unit masonry [2 full-scale concrete brick walls in Type N mortar and 2 wallettes in lime mortar – 1 historic brick and 1 concrete brick]. Typically, cracking began shortly after 9 hours and ultimately produced an average crack length of 418mm per hole and an average maximum 5.22mm crack width. Samples in Type-N mortar exhibited slower but significantly more cracks and wider cracking. Ninety-three percent of cracking occurred within 4 days. No masonry units were damaged and partial demolition was successful, although selective unit removal was not due to confinement.

Keywords: Soundless Chemical Demolition Agent, Historic Structures, Cracking, Masonry Structures, Expansive Cement, Unit Masonry, Concrete Brick, Mortar

1 INTRODUCTION

Soundless Chemical Demolition Agents (SCDAs) have shown to be a reliable alternative to traditional demolition methods like jackhammers and explosives for the demolition of rock and existing concrete structures near historic structures, environmentally sensitive locales, and densely populated areas. SCDAs achieve this through slow and localized material expansion of inserted material induced by a chemical reaction. To date, SCDA research has focused on concrete and rock removal but not that of unit masonry, with no information available about selective demolition or removal of individual masonry units. Such targeted removal activities are often undertaken when specific masonry units are damaged and need replacement or when historic materials are to be harvested for reuse, as was done in the large-scale $20 million rehabilitation of the Jacob Riis bathhouses in New York City where one of the two bathhouse structures was used to reclaim original material for the restoration of the other bathhouse (Fig. 1) [Gleeson, 2018]. The reclaimed material involved interior and exterior clay brick and glazed ceramic wall tiles. In that project, thousands of units were removed via mechanical means, and numerous units were chipped, cracked or broken during the noisy and labor intensive extraction process.

Presently, while there is guidance for concrete and rock demolition with SCDAs, in those applications, the drill hole for SCDA application is oriented perpendicular to the ground surface (usually vertical), and the size and placement of the drill holes are not strongly constrained by the configuration and composition of the material to be removed. This is in strong contrast to unit masonry where drill holes would need to be horizontally oriented and only placed at intersecting mortar joints if one of the objectives was to preserve the masonry units. As such, guidance is needed with respect to drill hole sizing, quantity, and distribution. In addition, little is known with regard to the general mechanisms for crack propagation under such conditions or even if cracking of the masonry units

can be avoided. To begin to fill these gaps, this paper explores the demolition of unit masonry in a laboratory environment through the selective application of a commercial SCDA.

Fig. 1. Half of Jacob Riis Bathhouse Used as a Source for Masonry Unit Reclamation for a Full Restoration of the Mirrored, Counterpart Structure further up the Beach.

2 BACKGROUND

Most SCDAs are grayish, powdery, dry materials similar to Portland cement, but with a higher percentage of calcium oxide (CaO). Other substances like ferrous oxide (Fe_2O_3), magnesium oxide (MgO), aluminum oxide (Al_2O_3), silicon (SiO_2), Portland cement, clinker materials, and calcium fluoride (CaF_2) have been added to change, enhance, postpone, or control the hydration procedure (Hinze and Brown 1994). Mixing an SCDA with water produces an exothermic chemical reaction of calcium oxide (CaO), which generates heat and expansive pressure. To categorize this exothermic reaction, Goto et al. (1988) proposed Equation 1:

$$CaO + H_2O \rightarrow Ca(OH)_2 + 15.2 \uparrow (kCal/mol) \quad (1)$$

Depending upon the SCDA type, volume, and surrounding conditions, SCDA hydration heat can exceed 150°C, which can cause the mixture's free water to boil creating a blow out of the SCDA (Natanzi et al. 2016a). Under more controlled conditions, the hydration heat initiates volumetric expansion, which translates to radial outward pressure from the center of the SCDA insertion. After a certain period of expansion, the generated tensile stress exceeds the tensile strength of the surrounding material. At that point, cracks began to form on the hole's perimeter (Fig. 2). These cracks result from tensile stresses oriented at a right angle to the crack and compressive stresses aligned parallel to the crack direction. In the case of two or more holes, cracks propagate by tensile stress between the holes, as shown in Fig. 2. The extension of crack propagation could be influenced by controlling the tensile stress field around the drill hole, which could be designed based on the number and pattern of drill holes (De Silva et al., 2019).

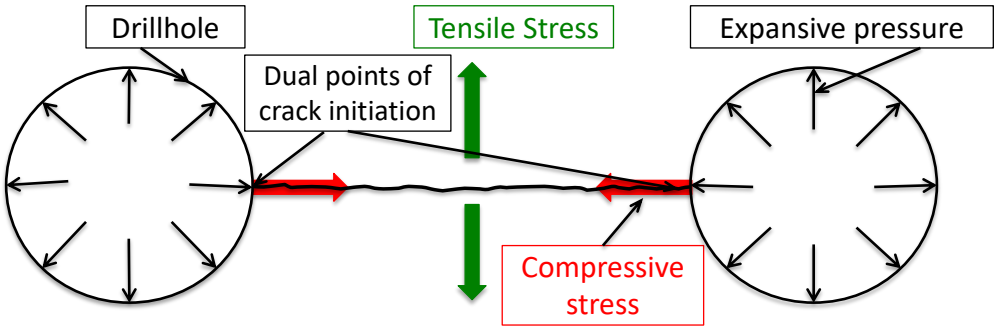

Fig. 2. SCDA demolition mechanism in two drill holes (adapted from Goto et al. 1988)

Characteristics of the holes in which the SCDA are introduced (e.g. diameter and spacing) play a notable role in SCDA performance and can reduce the demolition cost and improve demolition procedures. For example, surrounding material fracture toughness, the hole diameter, and SCDA maximum pressure each play a role in optimizing hole spacing. If all other parameters are held constant, stronger materials require closer hole spacing to achieve similar cracking levels (Natanzi and Laefer 2014).

To look at this more systematically, Arshadnejad et al. (2011) proposed a numerical model to optimize hole spacing (S) [Eqn. 2] that took into account the SCDA expansive pressure (P), the tensile strength of the material to be demolished (σ_t), the drill hole diameter (D), and the fracture toughness of the material to be demolished (K_{IC}), as shown in Equation 2:

$$S = \left[-0.0888\left(\frac{P}{\sigma_t}\right)^2 + 1.0824\left(\frac{p}{\sigma_t}\right) - 2.1583\right]\frac{P^2D^2}{K_{IC}^2} \quad (2)$$

Previously Gomez and Mura (1984) proposed a model Ls=kD to find the optimal straight line spacing between drill holes (Ls) for a selected drill hole diameter (D), while k is an experimental coefficient based on physical properties of different rock type and calculated with Equation 3:

$$k = \frac{\pi}{\sqrt{8}}\left\{\frac{4\mu\mu^*(1+\nu^*)\omega}{[\mu(1-2\nu^*)+\mu^*]\sigma_c}\right\}^{\frac{1}{2}} \quad (3)$$

where
ω is the effective free expansion strain of Bristar (a commercial SCDA),
σ_c is the fracture tensile stress of the rock,
μ is the shear modulus of the rock material,
μ* and ν* are corresponding quantities of the Bristar filled hole.

Gomez and Mura (1984) experimentally determined k < 10 for hard rocks, 8 < k < 12 for medium hard rocks, 12 < k < 18 for soft rocks and concrete, and 5 < k < 10 for pre-stressed concrete. Arguably, k values for unit masonry structures would be significantly less, as the experimental tensile strengths (σ_t) for brick masonry for a wide range of standard mortar mixes has been reported to be in the range of 0.45-2.57MPa (Drysdale and Hamid, 1982).

Gambatese (2003) recommended k values (6 to 12) based on small-scale reinforced concrete specimens, similar to the range of 5-10 proposed by Gomez and Mura for precast concrete. Gambatese's samples investigated 3 different hole diameters (3.18mm, 4.76mm, and 6.35mm) drilled into 152mm * 152mm * 76mm thick concrete specimens having a strength of 20.7N/mm^2. The hole depth of 38.1mm was kept constant. The results showed that increasing the hole diameter lead to earlier crack development but did not necessarily provide a greater number of cracks between

injected holes (Gambatese 2003). Specifically, cracking was shown to develop with a drill hole depth to diameter (L/D) ratio ranging from 6 to 12 and hole spacing to diameter ratios (S/D) ranging from 4 to 10.

Huynh and Laefer (2009) recommended hole diameters of 30-60mm depending upon surrounding material, with spacing distances of 20-70cm and hole depths of 80-90% of the sample depth for standalone high strength concrete samples of up to $1m^3$. Hole depths 70% of the sample depth were sufficient to initiate cracking but not necessarily to complete cracking through the entire thickness (Huynh and Laefer 2009). Harada et al. (1989) showed that deeper holes generated earlier crack development and increased crack width.

Selection of hole spacing and diameter may have other implications. For instance, Dowding and Labuz (1982) reported that mechanical material removal time could be a function of drill hole spacing (S) and the hole diameter (D), with optimal removal time at S/D = 8 and optimal cost at S/D = 16 for concrete and natural rock. Harada et al. (1989) also found that when the distance from the hole to the free surface was half of the hole spacing, the demolition time was reduced by almost 3 hours. Additionally, Dessouki and Mitri (2011) proposed that large diameter holes generated faster cracking, which, according to new work by Laefer et al. (2018), appears to be a function of the quantity of SCDA, as opposed to the actual hole diameter. To date, the effect of hole spacing and diameter have not been investigated in unit masonry.

Hole pattern also plays a significant role in the time to first crack (TFC) and crack propagation. For example, Harada et al. (1989) compared hexagonal and square arrangements of 22mm diameter holes in high strength concrete slabs of 60cm * 70cm * 40cm thick (keeping the number of holes constant). The hexagonal hole pattern was more effective—initiating cracking faster (within 10.5-12.5 hours) and propagating cracks more thoroughly (achieving propagation between all holes). The square pattern produced cracks after 12-15.5 hours but failed to develop cracks between all holes. In research by Gambatese (2003), a grid of holes was used in small-scale reinforced concrete blocks (152.4mm * 152.4mm * 76.2mm thick). Three hole diameter sizes (3.18mm, 4.76mm, and 6.35mm) were tested as repositories for the SCDA. To investigate potential savings, in some of the tests not all of the holes were filled with the SCDA.

In preliminary work on SCDA application to unit masonry, Natanzi et al. (2016b) tested 4 different hole layouts in small wallettes (225mm * 665mm * 100mm). Holes were cast into the mortar joints in the wallettes with spacers, as part of the original construction. This was done in one of three patterns: (Case A) each intersecting point of the vertical and horizontal mortar joints; (Case B) every second intersecting point of the vertical and horizontal mortar joints; and (Case C) at joints along the major diagonals of the specimens (Fig. 3). The SCDA was placed in these largely horizontal holes in slurry form; as the wallettes were single-wythe, the holes were plugged with modeling clay to keep the SCDA from draining out of the wallettes prior to setting. The experimental results indicated that holes in a diagonal layout were most effective for faster and more complete demolition (Fig. 3c). That work also demonstrated that once cracking begins, unconfined units along the top or sides of the specimen could be removed by hand.

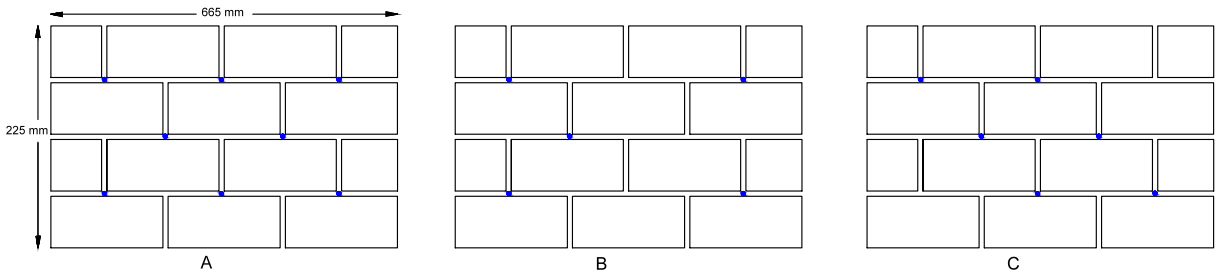

Fig. 3. Wall geometries and drill hole positions (Natanzi et al. 2016b)

Pilot work by the authors on concrete bricks showed that, depending on the SCDA type, temperature (ambient and mix water), hole geometry, and surrounding material, cracks may develop in as soon as a few hours or not until several days have elapsed. However, to date, unit masonry wall demolition with SCDA has not been systematically considered. This paper was designed as an initial step to overcome this knowledge gap through an experimental investigation into the selective and partial removal of unit masonry, which is an outgrowth of a preliminary study by the authors (Natanzi et al. 2016b), as will be elaborated in the Section 5.

3 METHODS

3.1 Scope

As many historic structures are composed of load-bearing masonry and are highly vulnerable to damage if exposed to traditional demolition methods, this study aimed to establish the viability of SCDA usage in a load-bearing masonry unit wall, particularly with respect to selective unit removal. Because of the high variability of historic materials (especially after decades, if not centuries of exposure), these initial experiments were initiated to comprehend the underlying cracking mechanisms and processes (e.g. cracking onset, formation, and propagation) and were conducted in a relatively controlled and repeatable environment. Single-wythe block structures were the focus of this experiment, as they represent almost 50% of all masonry buildings, and single-wythe, concrete block walls are one of the quickest, strongest, and most cost-effective building designs (Argila 2008), as well as being the basis for extensive finite element analysis and seismic investigation (e.g. Senthivel and Lourenco 2009, Dhanasekar and Xiao 2001, Gambarotta and Lagomarsino 1997). This experimental work was conducted with full-sized units across a limited spatial extent (with partial walls and wallettes) and changing the hole arrangements, mortar, and masonry units to explore the underlying mechanisms in SCDA demolition of masonry assemblages.

3.2 Materials

Two mortars mixtures and two types of solid masonry units were tested (Table 1). One mortar was a common Type N with typical 28-day compressive strength of 10.34–16.55MPa (ASTM International 2014a). The other was a lime-based mortar (with a typical compressive strength of 2.37 MPa), which was considered characteristic of historic 19th and early 20th century construction in Dublin, Ireland (Pavia et al. 2006). The compositions of the two mortars are shown in Table 2. The masonry walls and wallettes were comprised from either concrete bricks sourced from a local building supplier or historic brick. The historic bricks were salvaged and purchased from a local builder. Their yellow appearance closely matches those sold in the early 20th century from the Dolphin Barn brick. Details of the masonry units are provided in Table 3.

Table 1. Wall Configuration

Specimen	Size	Mortar*	Masonry Unit Type^	Hole layout	Masonry units (No.)	Drill holes (No.)
1	132.8cm x 128.6cm x 10cm	Type N	Concrete	Unit removal	72	8
2	132.8cm x 128.6cm x 10cm	Type N	Concrete	Diagonal	72	22
3	74.6cm x 88.2cm x 10cm	Historic Lime	Concrete	Unit removal	28	4

4	74.6cm x 88.2cm x 10cm	Historic Lime	Salvaged Brick	Unit re-moval	28	4

*See Table 2
^See Table 3

Table 2. Mortar Composition

Mortar Type	Materials			Water/ Binder	Sand/ Binder	Expected Compressive Strength (MPa)^
	Sand	Cement	Lime			
Type N	1	1	1	65%	6	10.34-16.55
Historic Lime	D10 = 10mm	0	3.5 NHL*	90%	2.5	2.37

*Naturally hydraulic lime
^See Table 4

Table 3. Masonry Unit Composition

Unit Masonry Type	Unit Size (mm x mm x mm)	Material	Condi-tion	Compressive Strength (MPa)
Concrete Aggregate Blocks	215 x 103 x 65	Cement-based	New	2.8
Historic	215 x 101 x 64	Clay-based	Salvaged	1.8

3.3 Masonry Prisms

For each wall or wallette, a prism was constructed contemporaneously for compression testing. Each prism consisted of 3 stacked masonry units (21.5cm * 10.2cm * 21.5cm) with 2 masonry bed joints, as per test Method B of ASTM C1314 (ASTM International 2014b). These were cured in the immediate proximity of the larger specimens. The mortar bed joint thicknesses, condition of units, and bonding arrangements replicated the larger assemblies. Compressive testing of the prisms occurred at 60 days, in accordance with Method B of ASTM C1314 (ASTM International 2014b). This coincided with the conclusion of the wall and wallette testing. Based on an expected compressive strength of 24MPa, a loading rate of 0.3N/mm^2/s was selected in accordance with Table BS in ASTM International (2014b). The average compressive strength of each sample is shown in Table 4. As expected, Specimens 1 and 2 had similar compressive strengths, as their constituent materials were the same. Specimen 3 was weaker than Specimens 1 and 2 and stronger than Specimen 4, as anticipated, because Specimen 3 had weaker mortar than Specimens 1 and 2 but strong units than Specimen 4. Specimen 4 had the lowest compressive strength, as the historic bricks and mortar were weaker than the component materials of the other specimens.

Table 4. Masonry Prism Compressive Strength at 60 Days

Prism Affiliation	Average Prism Compressive Strength (MPa)				Average Masonry Unit Compressive Strength (MPa)	Mortar Compressive Strength (MPa)
	1	2	3	Av.		
Specimen 1	13.97	14.08	14.01	14.02	2.8	10.34-16.55
Specimen 2	14.02	13.97	13.98	13.99	2.8	10.34-16.55
Specimen 3	10.24	10.69	10.39	10.44	2.8	2.37
Specimen 4	9.42	8.82	8.73	8.99	1.8	2.37

3.4 Wall Configurations

Type N mortar is a typical mortar used in the construction of the both exterior and interior load-bearing walls (ASTM International, 2014a) and was, thus, selected for the bedding material for the partial walls (Specimens 1 and 2). The wallettes (Specimens 3 and 4) were laid in historic, lime-base mortar (Table 2). In Specimen 3, this mortar was paired with the concrete bricks to begin to understand the role of the mortar in controlling the SCDA response. The larger concrete brick walls provided a control standard by which to investigate the cracking, as historic materials and their interactions are much more variable see Laefer (2001) and Laefer et al. (2004) for a discussion of this with respect to experimental design to replicate historic masonry.

The size of the historic brick wallette (Specimen 4 - 74.6cm * 88.2cm * 10cm) was controlled by the limited availability of the historic salvaged clay bricks and was 7 bricks high and 4 bricks wide. The other wallette, laid in lime mortar (Specimen 3), was constructed to match the size of Specimen 4 but included concrete bricks instead of the salvaged clay bricks. The two walls (Specimens 1 and 2) were as large as could be safely constructed in the available laboratory. They were 12 units high and 6 units wide (132.8cm * 128.6cm * 10cm) and were more representative of actual field conditions (Fig. 4a, 4b). They were four times larger than the 66.5cm * 22.5cm specimens (4 units high by 4 units wide) previously tested by Natanzi et al. (2016b), but still only about a third of the size of a full-sized wall. Wall construction followed standard industrial procedures with a moistening of all the bricks prior to their contact with the mortar to prevent mortar desiccation.

After erection, the specimens were each covered by a polyethylene sheet to retain the moisture during the curing process. This cover was removed after 28 days. The walls were left to cure in the laboratory for a total of 30 days prior to the introduction of the SCDA, which marked the first day of testing.

In the larger specimens (1 and 2), the materials were identical, but the hole layout and demolition objectives differed. Specifically, Specimen 1 (Fig. 4a) was constructed with 8 holes: 1 at each corner of the two selected bricks to attempt selective removal of a masonry unit in the upper and lower portions of a wall. The two locations were selected to explore the relative influence of confinement. In contrast, Specimen 2 (Fig. 4b) was constructed with 22 holes organized along 2 diagonals, as per the typical cracking patterns that occur in masonry walls under differential settlement. This layout was chosen to investigate the partial demolition of a masonry wall. The wallettes (Specimens 3 and 4) (Fig. 4c) were identical to each other in hole layout with 4 holes around the center masonry unit but differed in their material composition with Specimen 3 of concrete bricks and Specimen 4 of historic clay bricks.

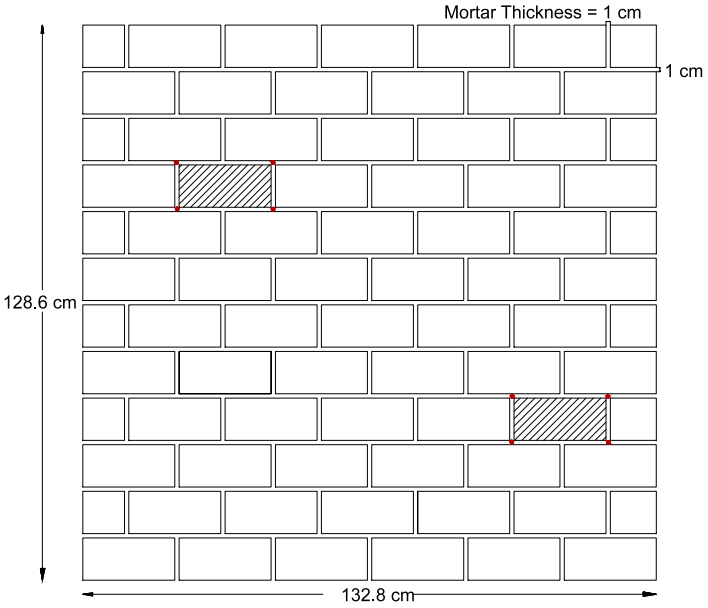

a) Layout of Specimen 1 for selective removal of two masonry units

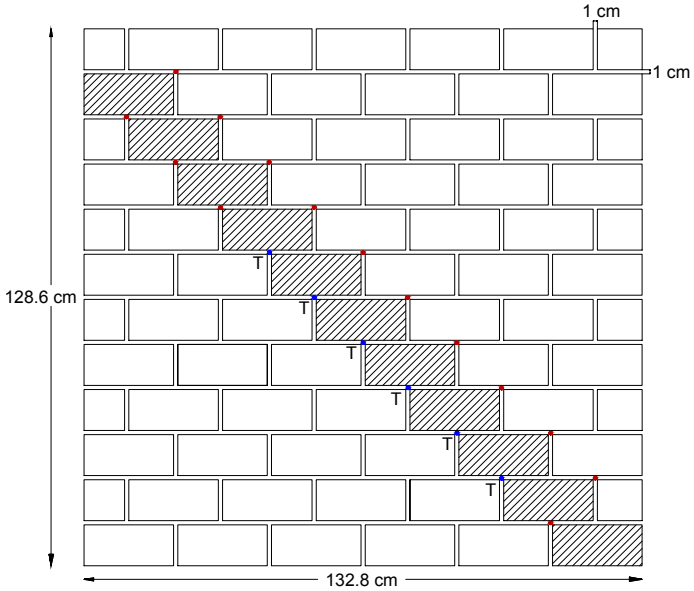

b) Layout of Specimen 2 for partial demolition

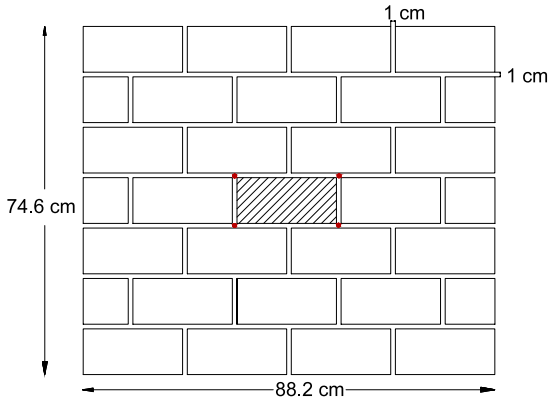

c) Layout of Specimens 3 and 4 for selective removal of middle masonry unit

Fig. 4. Schematic of specimens and testing arrangements with thermocouple locations for temperature monitoring in the SCDA labelled with T, other SCDA locations shown in red, and units selected for removal shown as hashed

After a minimum of 28 days of curing, the pre-specified 5mm diameter holes were drilled into the mortar joints according to the patterns shown in Fig. 4 with red dots. In contrast to previous, cast-in-place efforts (Natanzi et al. 2016b), this approach was a deliberate effort to begin to develop a viable field procedure for the application of SCDAs to vertical unit masonry walls. In the testing herein, the holes were cleaned with compressed air and then filled with Bristar 150, which, according to the manufacturer, is designed for temperatures up to 20°C. The Bristar was mixed according to the manufacturer's recommendations (tap water at 15°C; 30% by weight). The SCDA was injected under light hand pressure using a syringe with a 5mm diameter opening.

For three weeks after the injection, frequent monitoring was undertaken to track crack formation and propagation (by measuring crack lengths and widths), the time to first crack (TFC), crack length, maximum crack width, and a calculated average crack propagation speed (Table 5). Heat of hydration was monitored for almost a month with thermocouples inside the filled drill holes at six locations on Specimen 2 (shown in Fig. 4b as "T"). Thermocouples were restricted to Specimen 2 due to limited lab equipment.

Table 5. Test Monitoring Frequency

Day	Monitoring Frequency
1	Every 1 hour
2	Every 2 hours
3	Every 3 hours
4	Every 4 hours during the day and every 6 hours during the night
5	Every 6 hours
6	Every 8 hours
7	Every 8 hours
8-21	Every 24 hours

4 EXPERIMENTAL RESULTS

One of the major parameters reported by both SCDA manufacturers and researchers is the time to first crack (TFC), which was measured as the time elapsed from the SCDA injection into the drilled holes until a crack was visible near one of the drill holes. Another commonly reported parameter is crack length (L_{cr}), defined herein as the measurement at any particular time from the end of the crack to the edge of the drilled hole from which the crack originated. Cumulative crack length was considered as the total length of all cracks present in the specimen at the end of testing. This term is often reported in conjunction with a maximum crack width (W_{max}), which was considered as the maximum width among all cracks present at the end of the testing period measured in the direction perpendicular to the crack's direction of travel. A final commonly reported parameter is the average crack speed (V_{av}), which is the propagation rate of the crack extension in the direction of travel. A summary of the cracking results is presented in Table 6.

Table 6. Summary of Testing Configuration Results for Four Masonry Wallettes

Specimen	# of holes	Holes with cracks (%)	Av. # of cracks per hole	Total # of separate cracks	TFC (hrs)	W_{Max} (mm)	Max. Crack length (mm)	Cumulative crack length (mm)	Cracked / hole (mm)	V_{av} (mm/sec)
1	8	87.5	2	34	11	6.43	1104.1	3360.1	420	0.0035
2	22	100	3.18	63	9	10.76	594	7604.1	346	0.0081
3	4	100	3	22	10.2	NM*	109.6	1585.8	397	0.0092
4	4	100	3.25	17	8.5	3.67	213.8	2033.5	508	0.0118
Average			2.858	34	9.7	5.22	505.4	3645.9	418	0.0081

***Non-measurable**

4.1 Specimen 1

Cracks started to appear around the drill hole at the upper right corner of the target brick in the top left region of the wall after 11 hours (A in Fig. 5b), with cracking then appearing at the two B locations in the bottom right quadrant. The A symbol shows the boreholes at which the first cracks appeared in all figures. The greatest single crack length was 1104.1mm, which appeared in the lower portion of the wall 15 hours after the onset of testing (Fig. 5b, green color). After that time, only a few small cracks were generated and/or propagated. The maximum crack width 6.43mm, was located at the bottom of the specimen and was as part of the largest crack. The crack widths around the top block were too slight to be measurable with Vernier calipers (Fig. 5b). At the end of testing, the cumulative length of all cracks was 3360.1mm (17.7% of the available mortar joints).

Although cracking occurred near the units targeted for removal, the goal of selectively removing the masonry unit was not successful at either of the two locations. At the upper location, cracking around the target unit was incomplete (1 of the 4 holes developed no cracks). At the lower part, the wall was cracked entirely, but surrounding confinement was too significant to remove the masonry unit by hand (Fig. 5b, green color). That the lower portion of the specimen cracked more than the upper portion was unanticipated based on the higher level of confinement present at the bottom of the specimen. Notably, all cracking remained within the mortar joints.

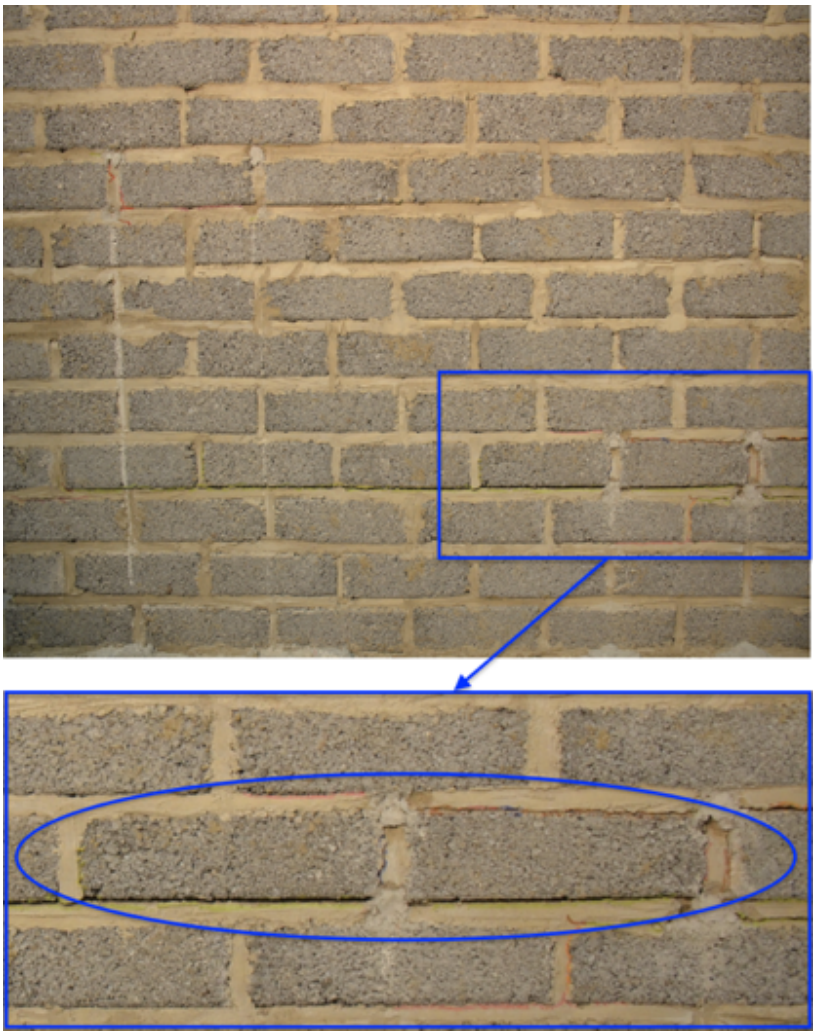

a) Crack propagation photo and close up

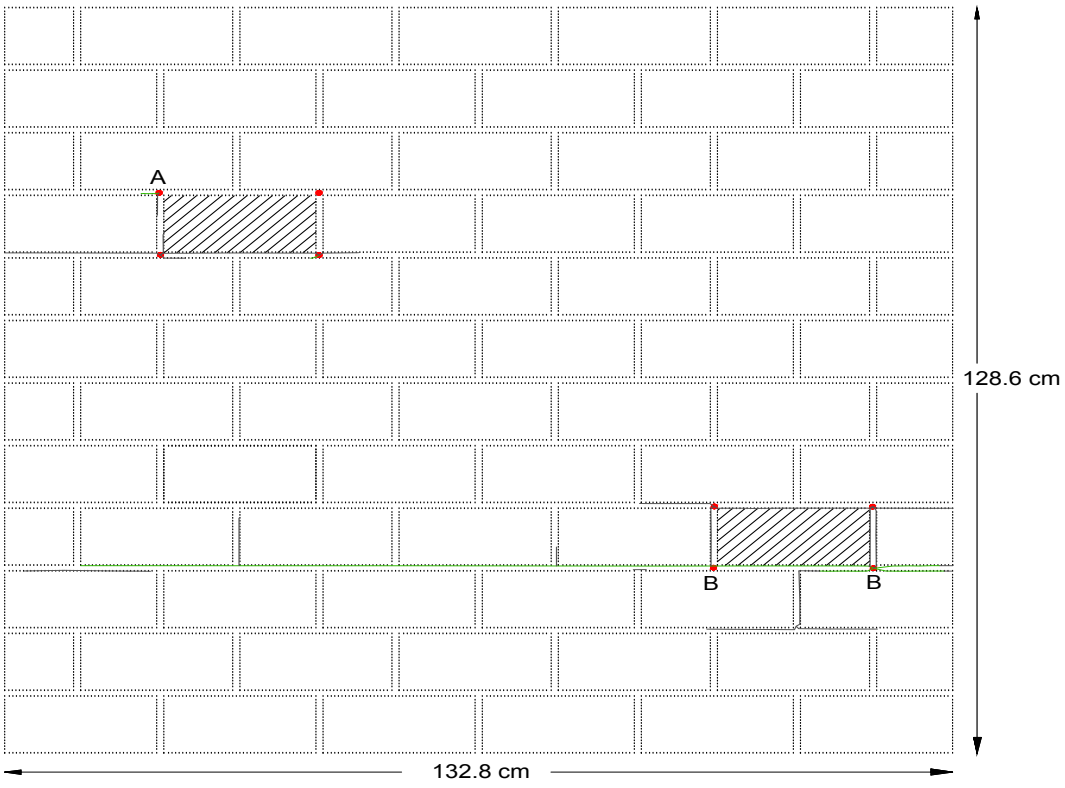

b) Crack propagation sketch

Fig. 5. Specimen 1 after testing

4.2 Specimen 2

Cracks started to appear in the upper part of Specimen 2 after 9 hours. The longest crack, which appeared near the middle of the wall, was 597mm. The widest crack was 10.76mm and was recorded at the top of the wall (location 1 on Fig. 6b), while the bottom of the wall had a maximum crack width of only 6.51mm. The cumulative crack length reached 7604.1mm at the end of testing (representing 40% of the available mortar joints).

Specimen 2 had the highest number holes (22) [red dots in Fig. 6b]. Each hole generated at least one crack and cumulatively produced cracking along the pre-designated diagonal pattern across the entire wall in two parallel bands. All units above the diagonal band could be removed by hand and without further damage to the units below the band (cross-hatch bricks in Fig. 6); Larger walls are likely to need more holes. There was also a small amount of unintentional damage in the top left-hand corner probably caused by the lack of confinement during the cracking process (green double cross hatched units in Fig. 6b). As with Specimen 1, all cracking was confined to the mortar joints.

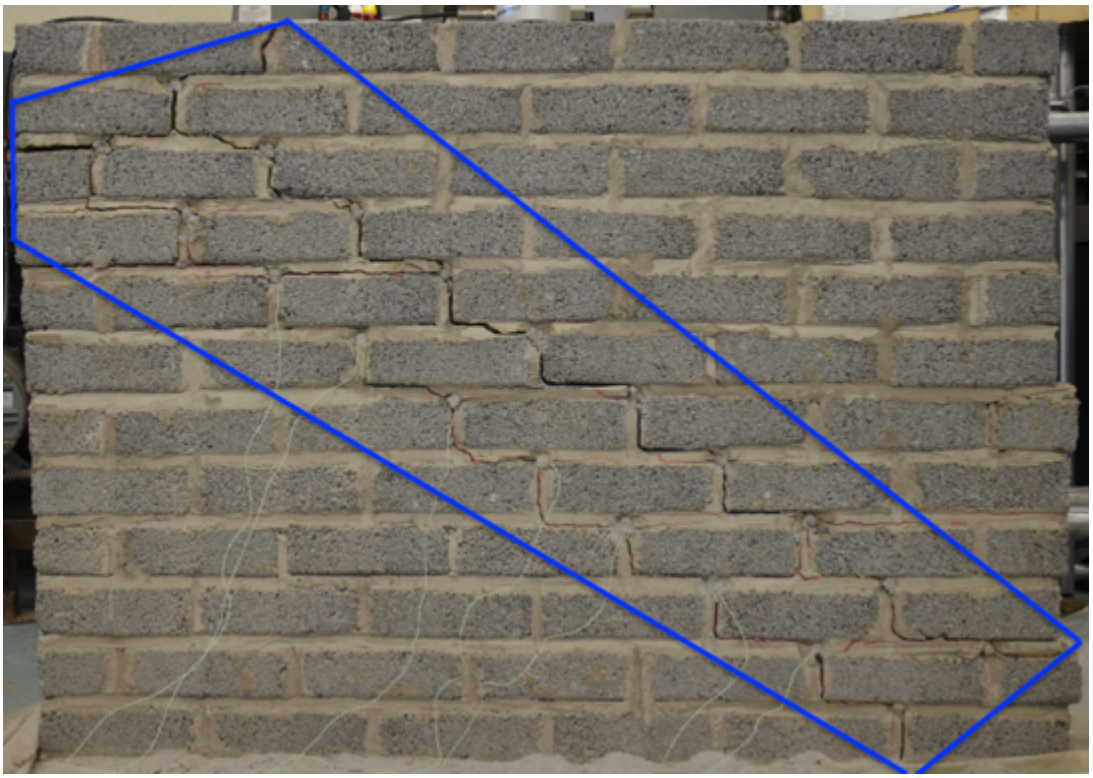

a) Crack propagation photo

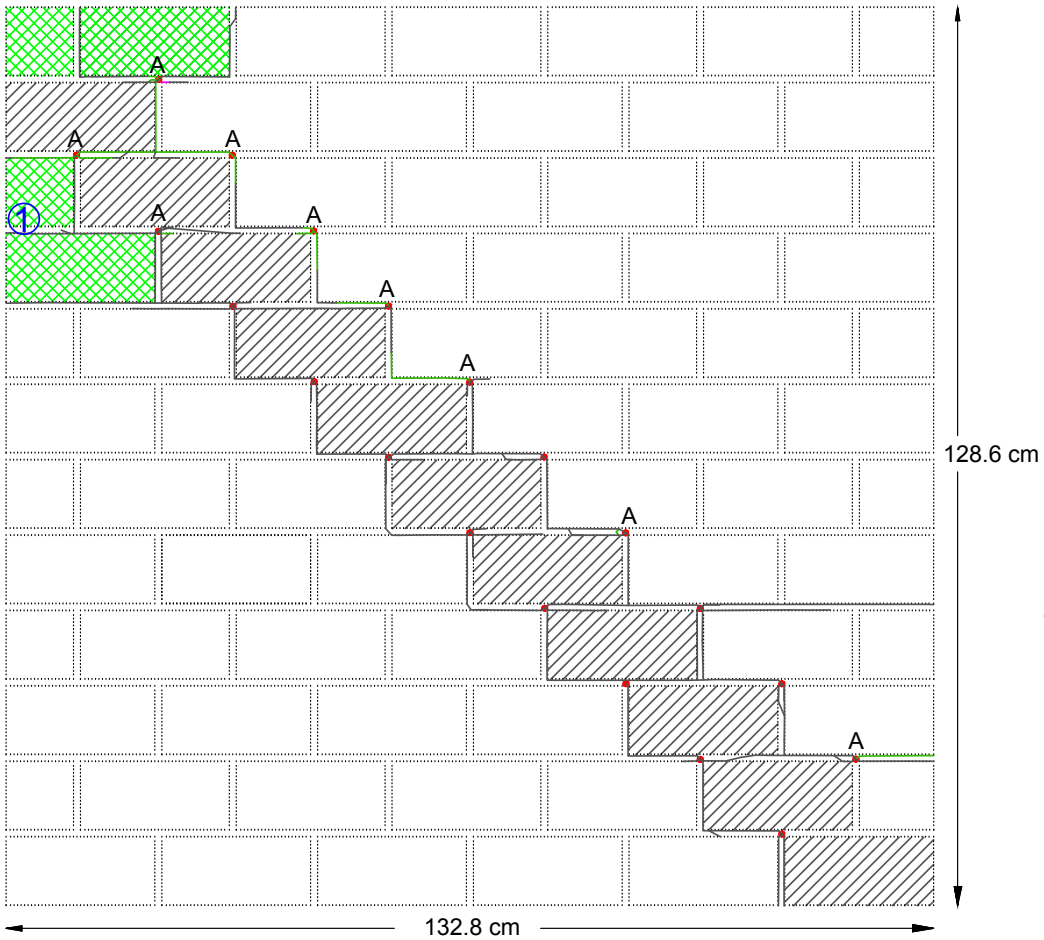

b) Crack propagation sketch

Fig. 6. Specimen 2 after testing

4.3 Specimen 3

In Specimen 3, micro-cracks started to appear around all holes 10.2 hours after SCDA injection. At the end of testing, the maximum crack length was 109.6mm, and the cumulative crack length was 1585.8mm (23.2% of the available joints), but the cracks were not sufficiently wide to be measured with Vernier calipers (Fig. 7b). Specimen 3 showed less cracking per hole than the other samples. The removal of the target unit was not possible, because cracking around the target unit was incomplete. Cracking was confined to the mortar joints.

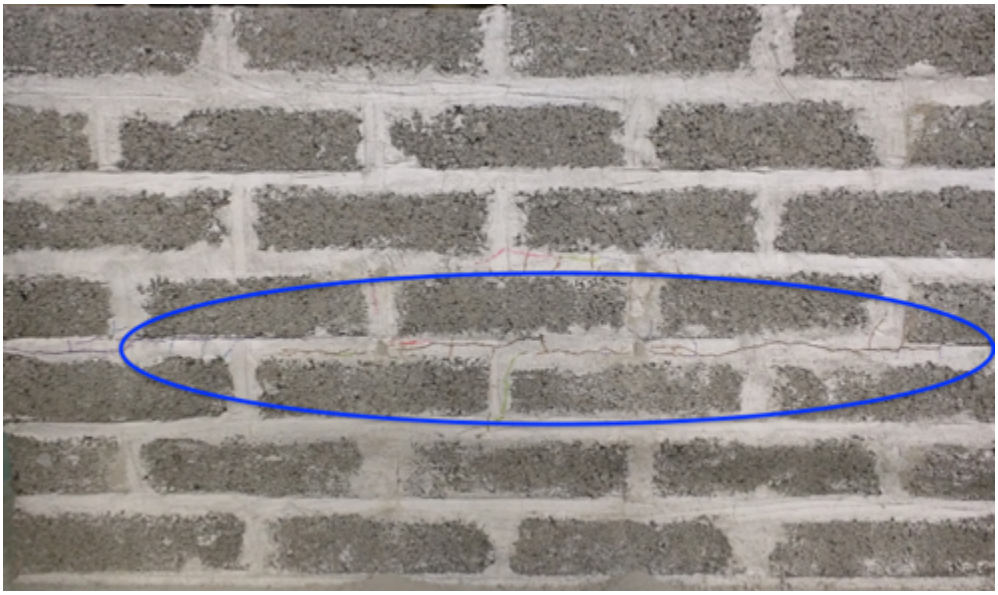

a) Crack propagation photo

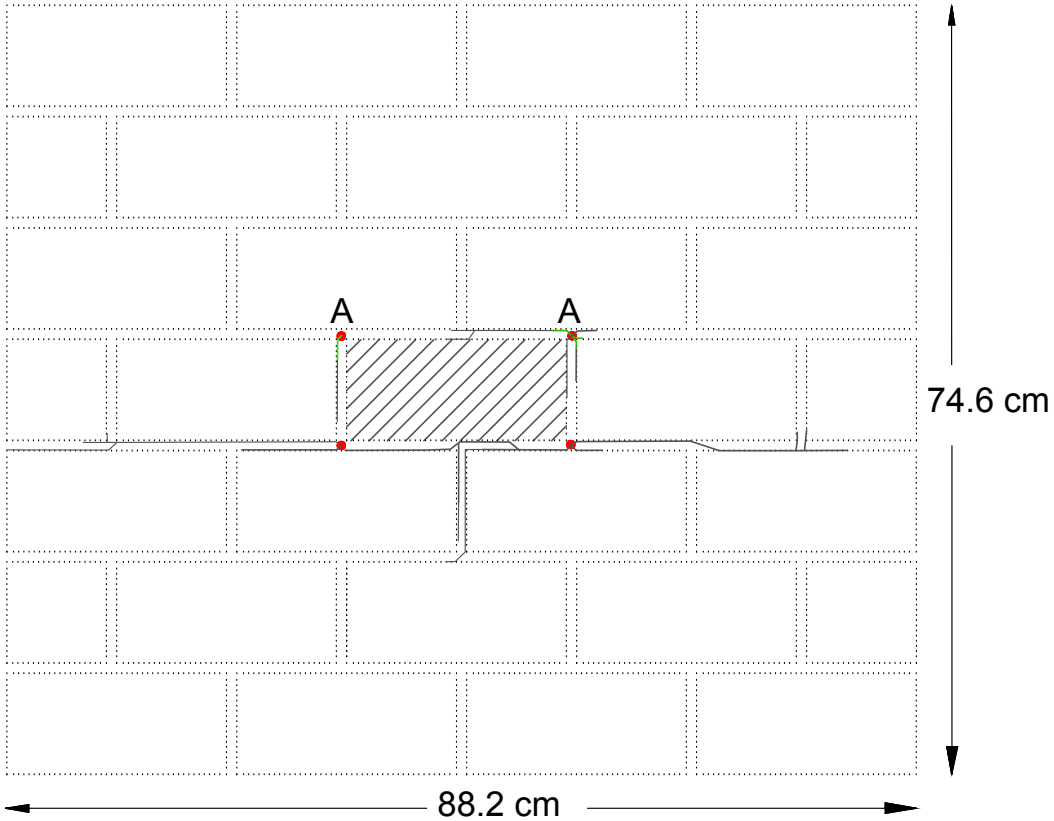

b) Crack propagation sketch

Fig. 7. Specimen 3 after testing

4.4 Specimen 4

In Specimen 4, cracks commenced 8.5 hours after SCDA injection (Fig. 8a). They first appeared around the upper drill holes and propagated horizontally around the drilled holes, ultimately reaching a maximum crack length of 213.8mm. A maximum crack width of 3.67mm was recorded at the middle of the wall. A cumulative crack length of 2033.5mm (29.8% of the available mortar joints) was recorded at the end of testing (Fig. 8b).

As illustrated in Fig. 9a, experimental results showed that the greatest rate of crack generation occurred within the first week, during which the ambient temperature ranged from 17-23°C. In the first 4 days, 93% of the total, final crack length was achieved, after which cracking slowed noticeably (Fig. 9a). For each specimen, the majority of the cracking happened between days 1 and 2. At the end of two weeks, the cumulative crack length was highest in Specimen 2 and lowest Specimen 3 (Fig. 9b). In this specimen, like all other cases, the cracks appeared only in the mortar joints, and the units remained wholly intact.

a) Crack propagation photo

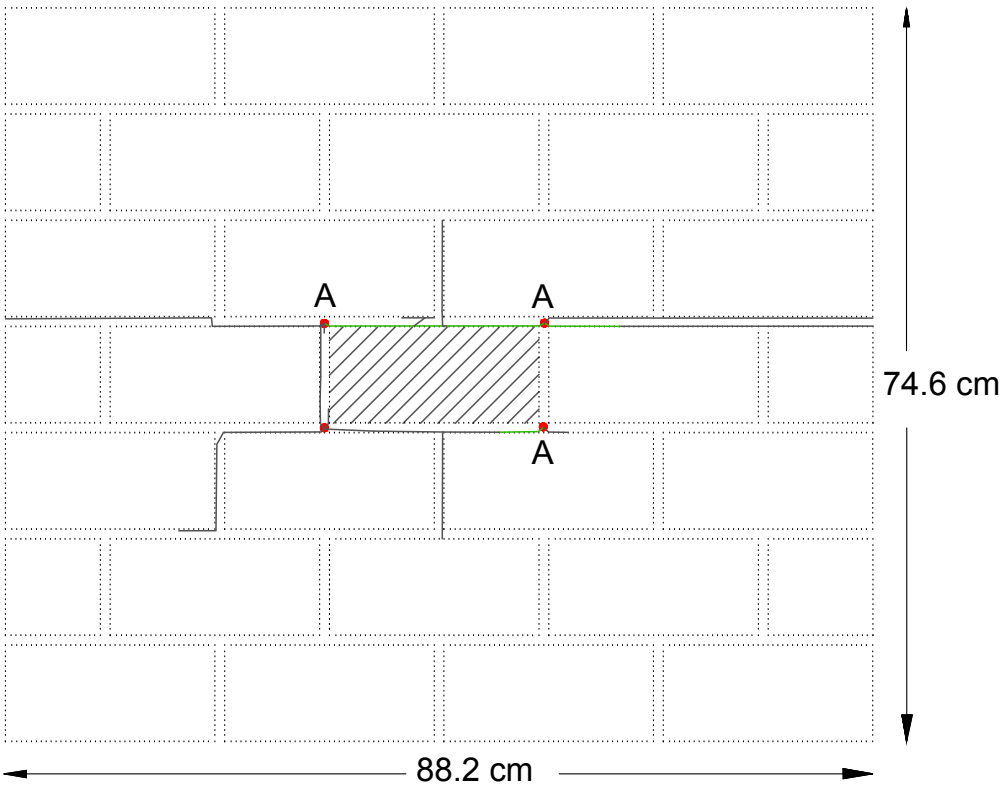

b) Crack propagation sketch

Fig. 8. Specimen 4 after testing

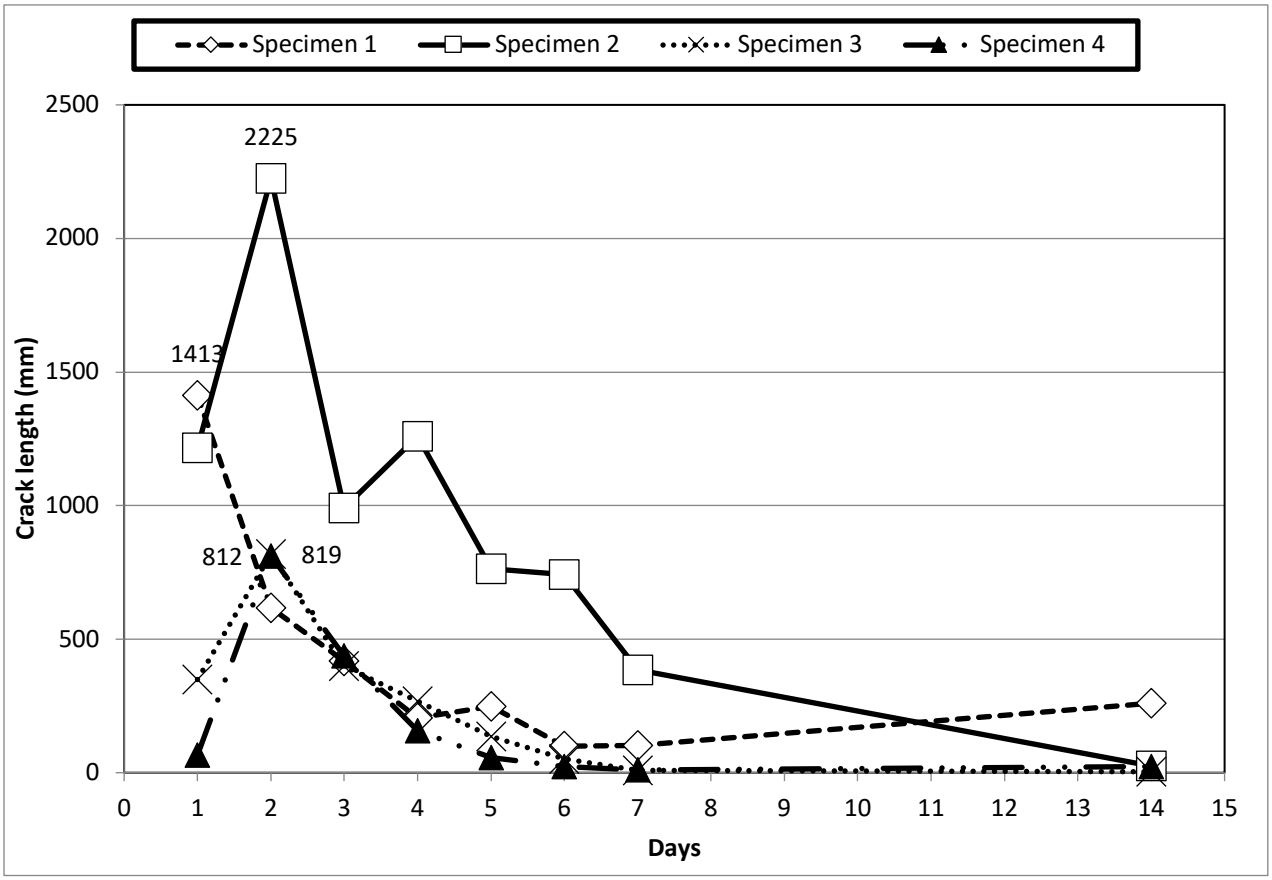

a) Crack length propagation during two weeks of testing

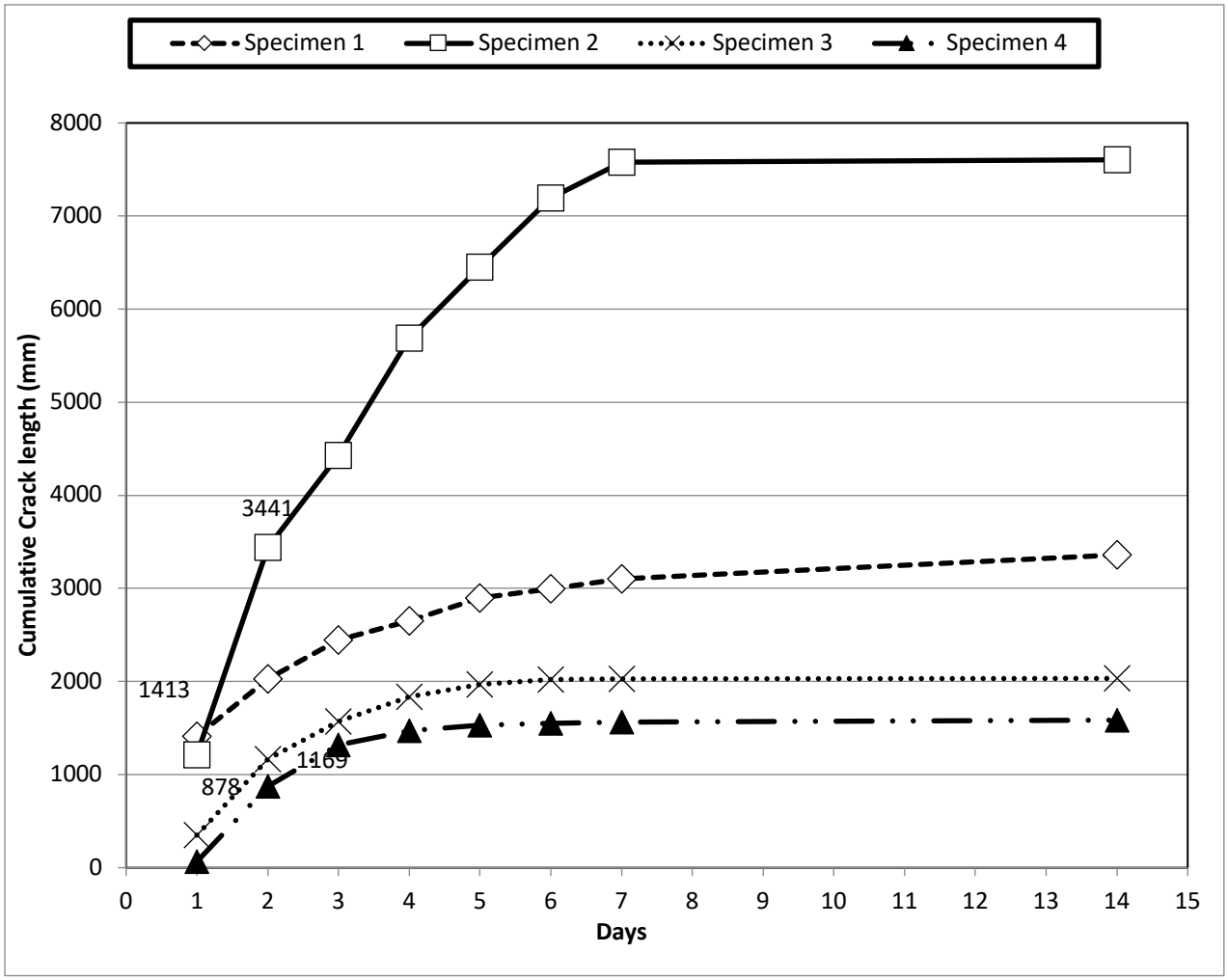

b) Cumulative crack propagation during two weeks of testing

Fig. 9. Crack length propagation in the four specimens

As summarized in Table 6, the SCDA performance was in many ways highly consistent irrespective of the walls' constituent materials. For example, among the 38 holes across the 4 specimens only 1 did not initiate a crack. Similarly, cracking in each specimen began within 12 hours. Distinctive behaviors between specimens were easily attributable to differences in the mortar. The stronger, more brittle Type N mortar of Specimens 1 and 2 exhibited significantly wider maximum crack widths (6.43mm and 10.76mm for Type N versus only 3.67mm and a non-measurable crack width in the lime mortar). However, cracking in the Type N mortar was slower (0.0035mm/s and 0.0081mm/s in Specimens 1 and 2, respectively, versus 0.00918mm/s and 0.01177mm/s in Specimens 3 and 4, respectively).

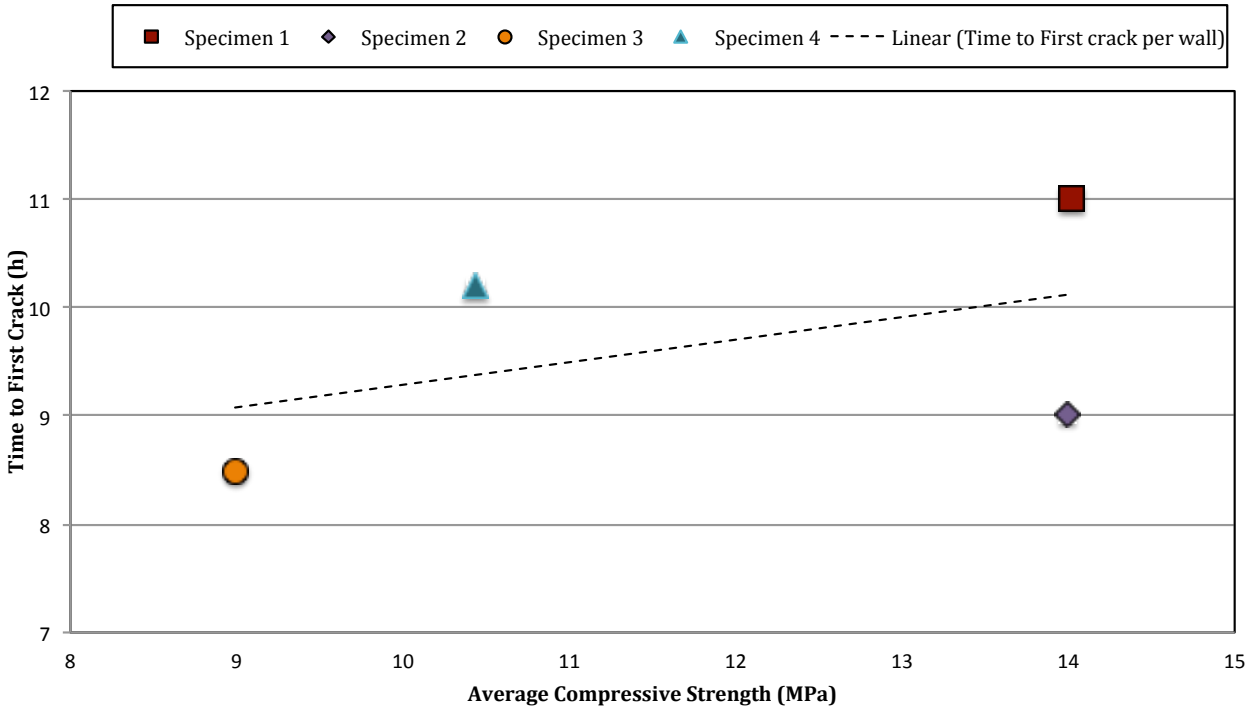

a) Time to first crack

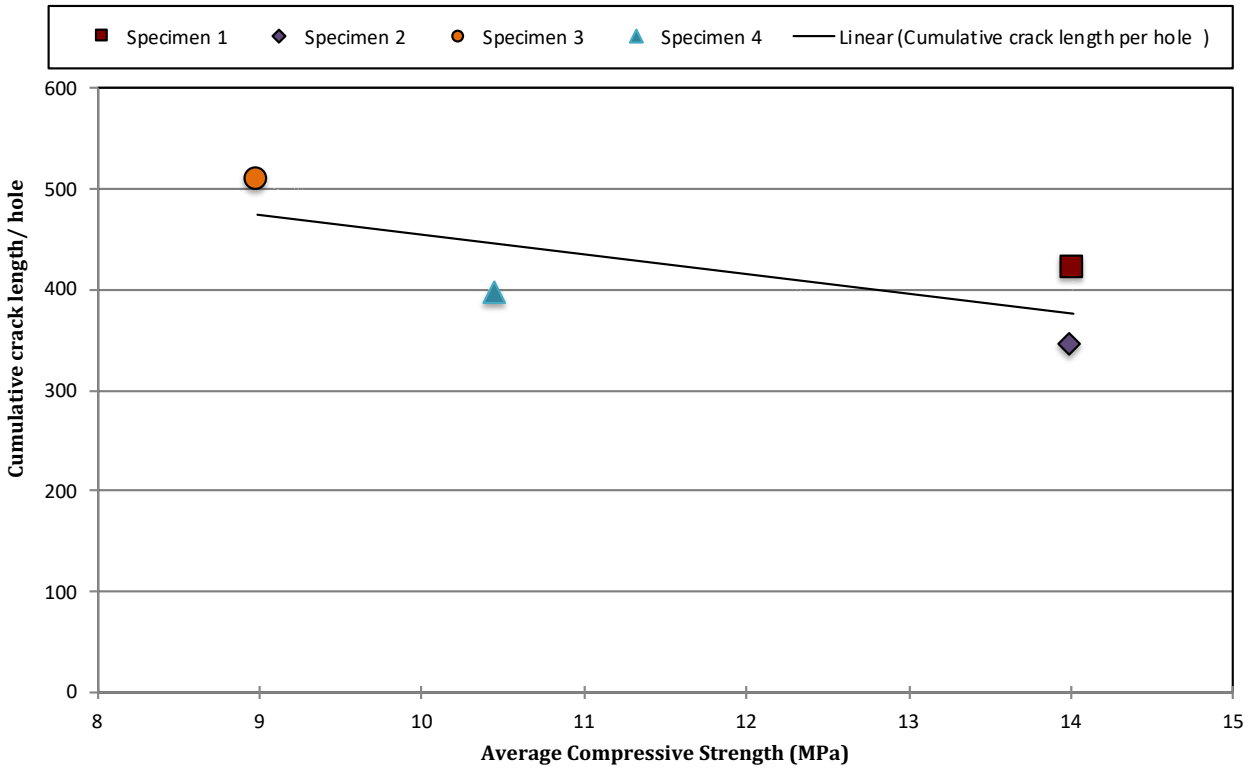

b) Crack propagation

Fig. 10. Time to first crack and crack propagation in different strength walls

Different hole patterns also significantly influenced the demolition. More holes meant a greater amount of injected SCDA, which resulted in greater expansive pressure generation across the specimens and, in turn, greater total crack lengths. In Specimens 1 and 2, which had the same masonry composition but a different hole layout, cumulative crack length in Specimen 2, with its 22 holes,

was double that of Specimen 1, which had only 8 holes. Time to first crack was also 2 hours faster in Specimen 2 than Specimen 1. When the hole pattern was identical (Specimen 3 and 4), the materials controlled the difference in the demolition process. Namely, Specimen 3 with the stronger masonry units (2.8MPa versus 1.8MPa), started to crack 2 hours later than Specimen 4, and Specimen 3 had a non-measurable final crack width versus 3.67 mm in the weaker Specimen 4. Overall, the TFC was shortest in Specimen 4, with its weaker mortar and salvaged bricks. Specimen 4 also had the greatest overall cumulative crack length per hole (Fig. 10b). As the materials in Specimens 1 and 2 were identical, Fig. 10b also shows the potential variability achieved where only the number of holes and their distribution changed. Similar disparities were shown previously in the work by Natanzi et al. (2016b). As an additional note, generally, the TFC was faster and the cumulative crack length per hole was higher in the specimens of lower strength (Specimens 3 and 4 in Fig. 10).

Results also showed that confinement could influence the demolition outcomes. In Specimen 2, the low level of confinement at the top resulted in a small amount of unintentional demolition. In Specimen 1, the results were less conclusive, as previously noted.

4.5 Temperature

As noted in the testing methodology section, only Specimen 2 was monitored for temperature. Temperature was monitored at 6 of the SCDA insertion locations, as well as in the ambient environment. Within all monitored drill holes, the temperature started to increase almost immediately, but cracking only began after 9 hours (Fig. 11). In the first 14 days, SCDA temperatures exceeded the ambient temperature by 1-2°C (Fig. 12).

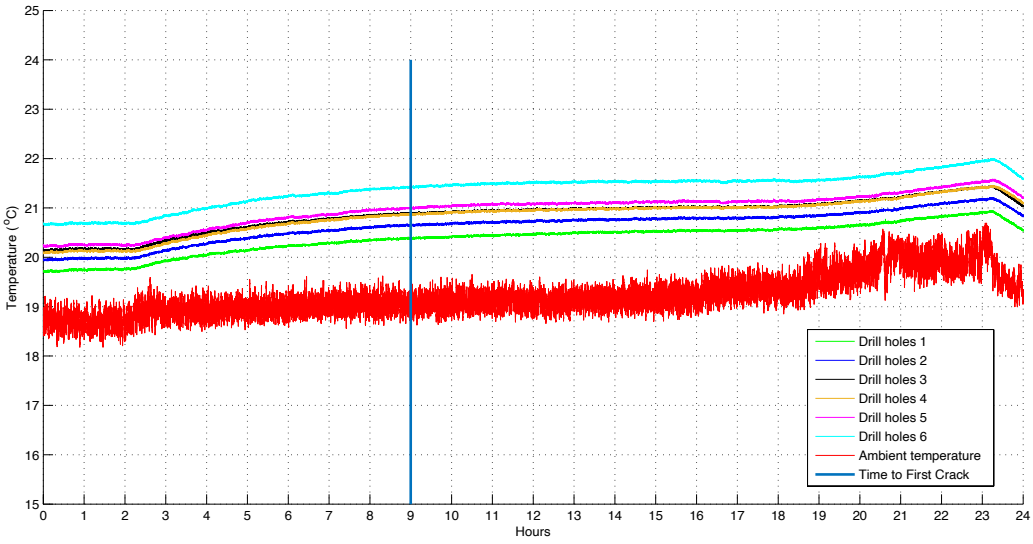

Fig. 11. Day 1 heat of hydration inside holes in Specimen 2 as compared to ambient temperature

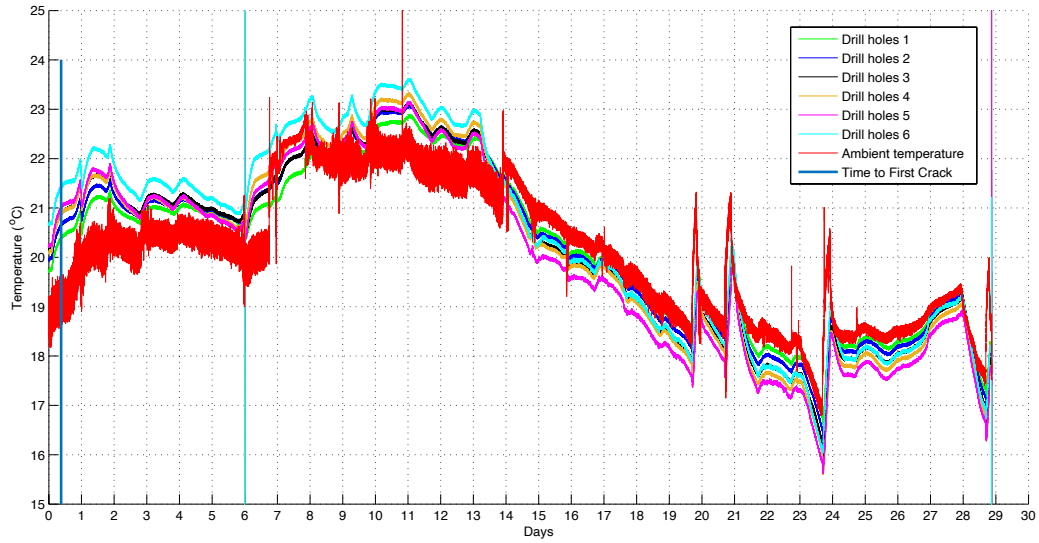

Fig. 12. Heat of hydration inside holes in Specimen 2 as compared to ambient temperature

While the gross temperature trends in the SCDA followed the ambient temperature pattern (Fig. 11), a closer look at the data showed a high degree of independence (Fig. 12). As the ambient temperature was uncontrolled and allowed to fluctuate, this test provides insights as to the heat being generated in these very small holes was influenced by the macro-environment. After 14 days, SCDA temperatures were lower than the ambient temperature, thereby implying that the hydration heat generation process was complete. A small amount of cracking, however, continued for up to 7 more days. Similar extended cracking was also reported by Hyunh et al. (2017) in large concrete blocks under equivalent environmental conditions.

5 DISCUSSION

Based on the above reported results several observations can be made about the application of SCDA to unit masonry with respect to the effects of the following parameters: (1) drill hole patterns in the mortar joints, (2) mortar and masonry unit strength, (3) hole spacing, and (4) hole diameter.

5.1 Drill hole pattern

The experiments reported herein showed the usefulness and high level of effectiveness of a diagonal drill-hole pattern in unit masonry. In work by Natanzi et al. (2016b), in much smaller unit masonry wallettes, this issue was explored explicitly under 4 different drill-hole layouts (red dots in Fig. 13). That work demonstrated that the pattern in wall D (Fig. 13) had a 70% higher than average cumulative crack length when the holes were in a diagonal pattern as compared to the other hole arrangements that were tested (Fig. 13 Walls A-C versus D). Normalizing the cumulative crack length by the number of holes, Natanzi et al. (2016b) showed a 362.09mm cumulative crack length per hole. Similarly, in the study herein, the diagonal layout had a normalized cumulative crack length of 345.64mm per hole for masonry of a similar strength (14.85MPa versus 13.99MPa) tested in the same temperature range (18.7-22.5°C versus 17-23°C). Previously, Harada et al. (1985) reported that the location of the drill holes greatly influenced the time to first crack during an experiment in high strength concrete slabs (4.21MPa; 60cm * 70cm * 40cm) in which a hexagonal layout of 22mm holes cracked 3 hours earlier than a planar layout with the same number of drill holes (Fig. 14).

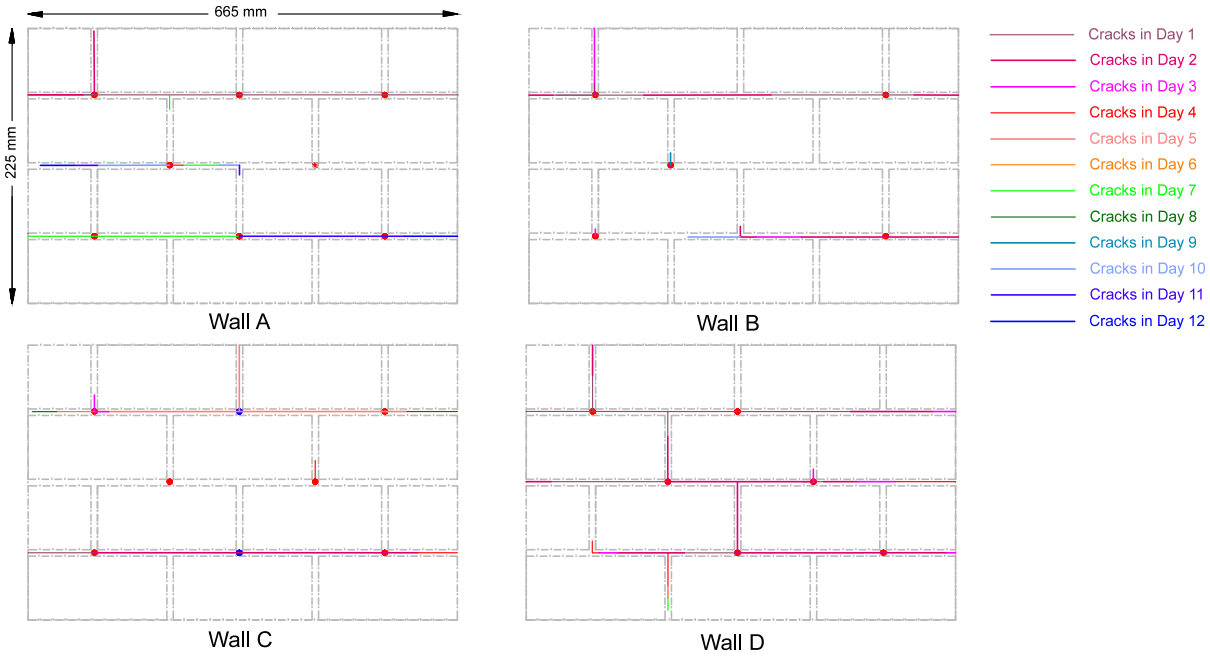

Fig. 13. Wall crack patterns (adapted from Natanzi et al. 2016b)

Notably, the work herein constrained the possible hole patterns by using only joint intersections as locations for drill holes. However, based on the work by Laefer et al. (2010) in large concrete blocks there may be justification for reconsidering this approach as the placement of drill holes in more confined locations (i.e. in the mortar joint but not at points of joint intersection) may facilitate more concentrated directional cracking. Moreover, more drill holes would increase the strain energy by lateral expansion and lead to greater fracture development as demonstrated by De Silva and Ranjith (2019) where the presence of more drill holes increased the proportion of shear fractures.

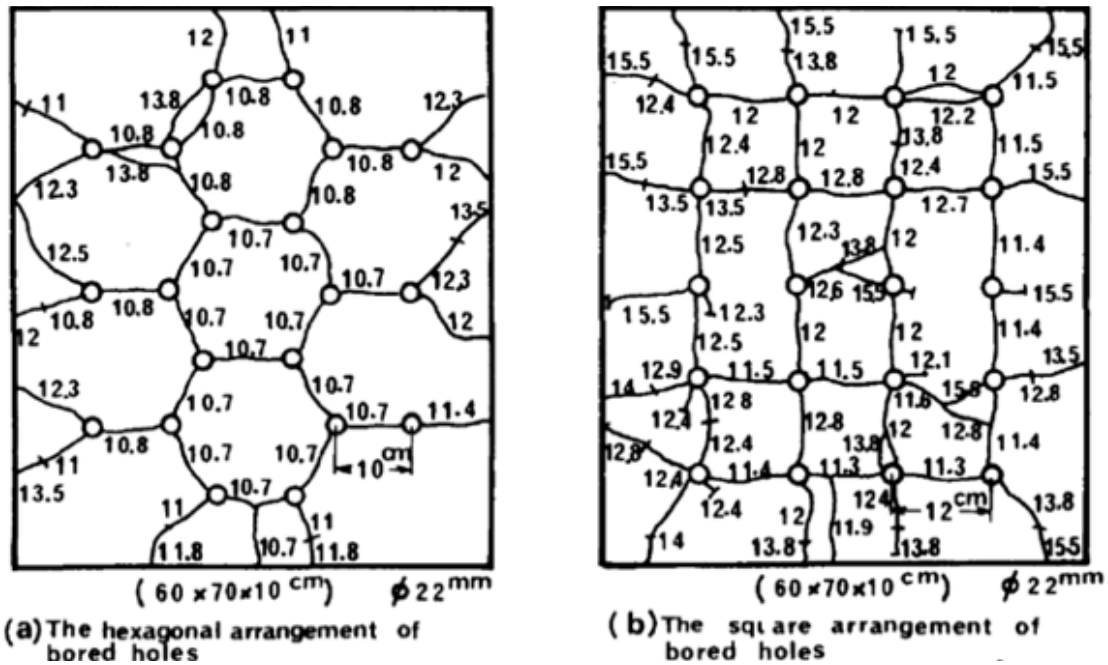

Fig 14. Borehole arrangement in Harada et al. (1985)

5.2 Material Strength with Respect to Time to First Crack

The SCDA manufacturer Bristar advises a time to first crack of 10-20 hours depending on the construction, environment, and material properties. In work by Gambatese (2003) in small concrete blocks with hole diameters of 3.18mm- 6.35mm cracks appeared after 12 hours. In a study on small unit masonry wallettes by Natanzi et. al (2016b), cracking began in the range of 9-17 hours across the 4 specimens (average strength 14.85MPa) with an average time to first crack of 12 hours (Fig. 13). In the research herein, cracks were observed 8.5 hours after SCDA injection, with cracking starting in all specimens no later than 12 hours after injection and typically around 9 hours. Crack propagation for the tests conducted herein are shown in Figs. 15-18 (red dots denote drill hole locations).

In the experimental research herein, the TFC was fastest in Specimen 4 with the salvaged bricks, which had the lowest compressive strength of the specimens (Fig. 10). While the SCDA manufacturer predicted expansion completion after 16 hours, the research herein demonstrated that mortar continued to crack for up to 3 weeks (albeit at slower rates). This was also observed by Huynh et al. (2017) in experimental testing of $1m^3$ unreinforced concrete blocks. Research by Tang et al. (2017) showed that the TFC is a function of the mortar stiffness and heterogeneity based on the simulation of crack initiation and propagation assuming a Weibull distribution. In that work, In heterogeneous materials like mortar exhibited two types of crack generation – high stress and low strength, where crack generation may start at a point where the stresses are not the highest but where the local strength is lower because of the effect of pores and micro cracks. If the material is completely homogeneous, failure initiates at locations of high stress (Tang et al. 2017). When using SCDAs in concrete or rock, the slurry is often introduced into the drill holes at the end of the day's work shift, with the expectation that material removal could begin at the onset of the morning shift 16 hours later. Because of the significantly small amount of SCDA material that can be introduced, the timeframe of a weekend may be more appropriate. Conversely, like with the rock removal done beneath the Carnegie Hall concert facility (Natanzi and Laefer 2014; Laefer 2002), in-situ material removal could be done progressively. In that case, efficient removal of the hundreds of tons of material was predicated on have an open face into which the cracked material could expand. Similarly, the partial demolition of walls may need a phased approach and should, along with multi-wythe construction be the subject of future tests.

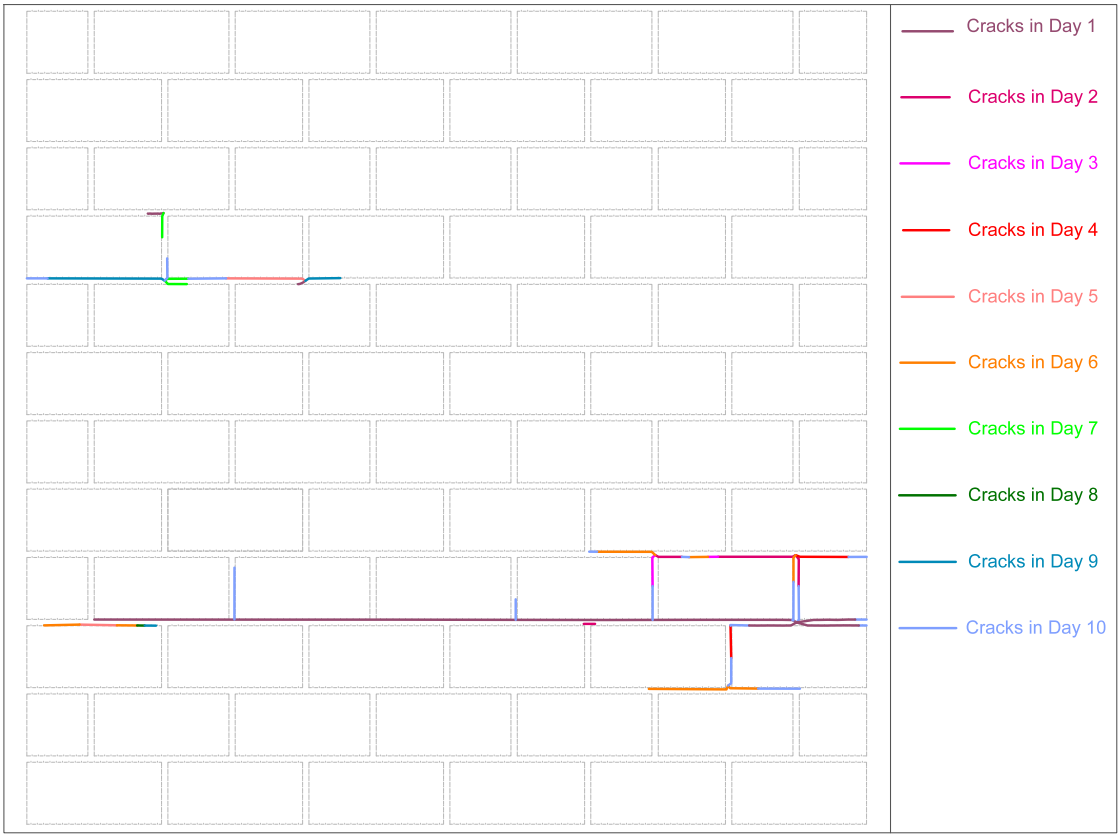

Fig. 15. Wall 1 crack propagation

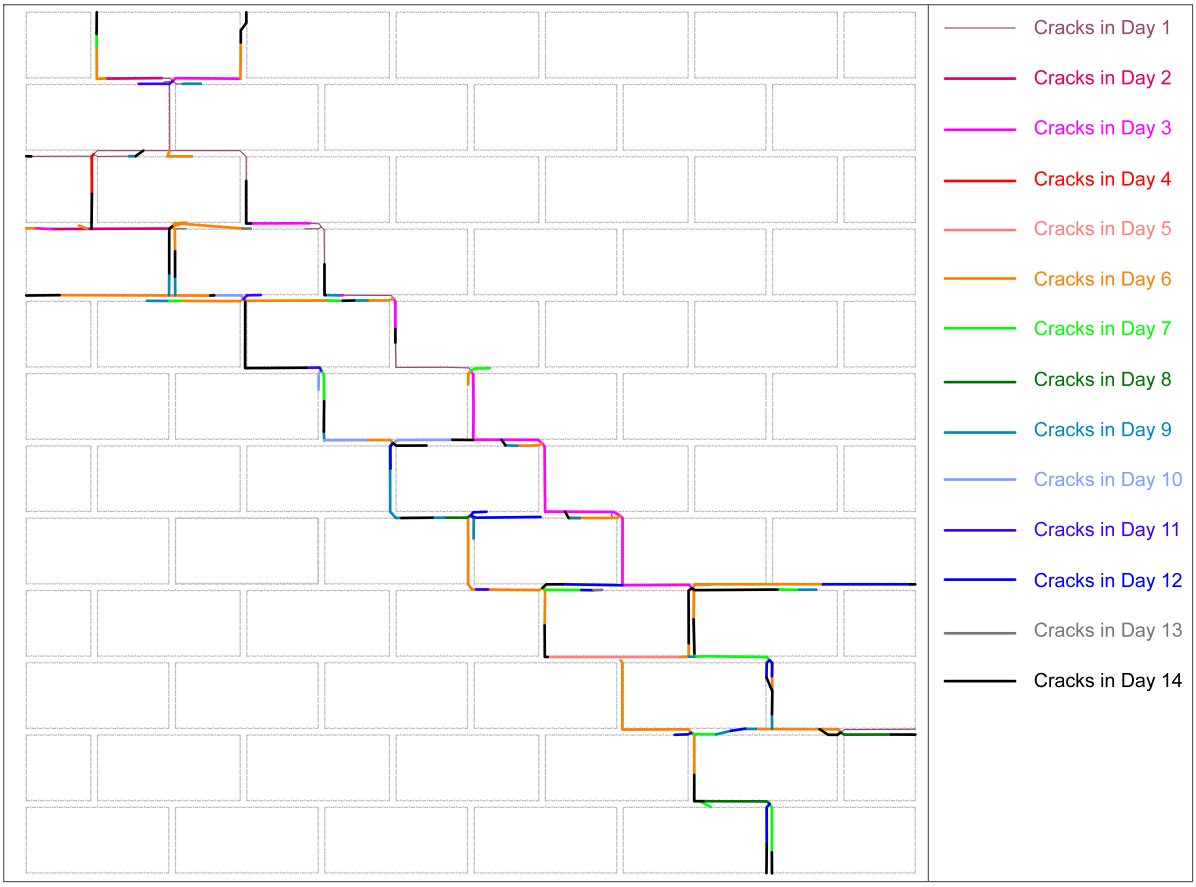

Fig. 16. Wall 2 crack propagation

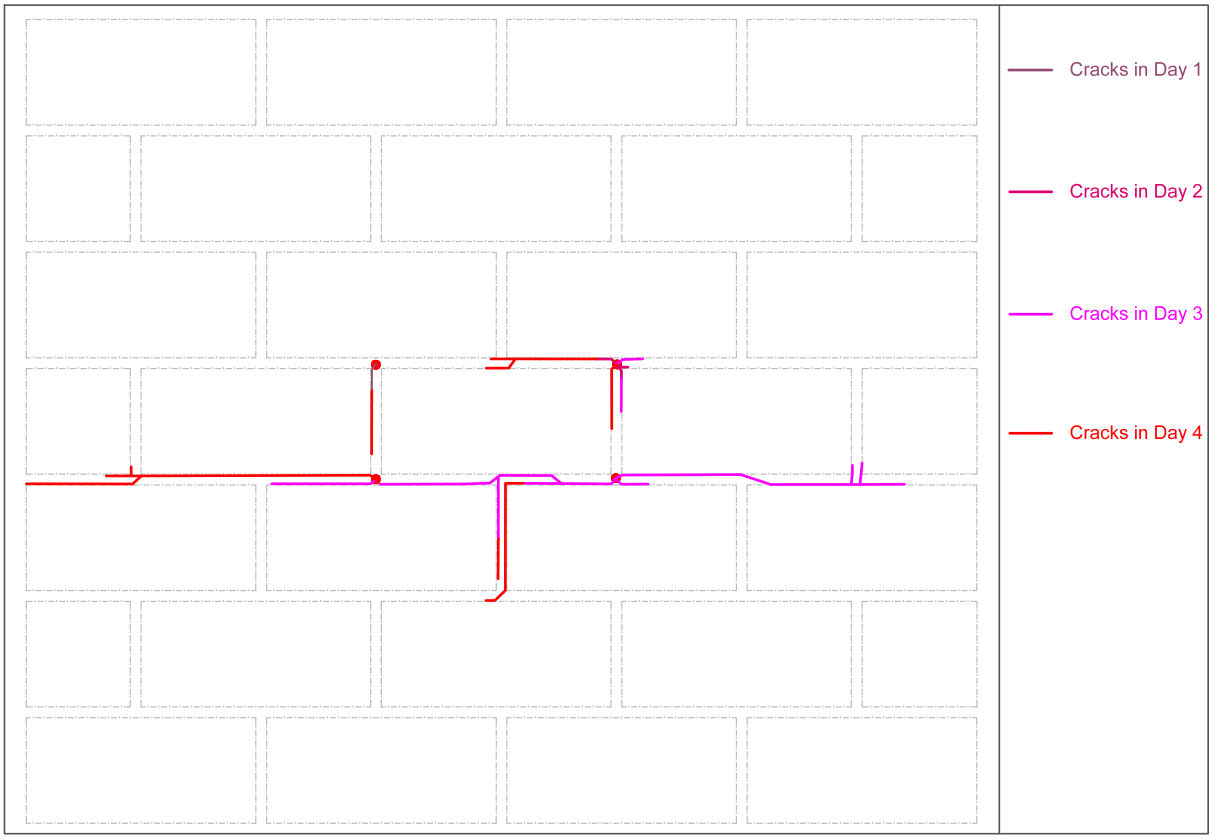

Fig. 17. Wall 3 crack propagation

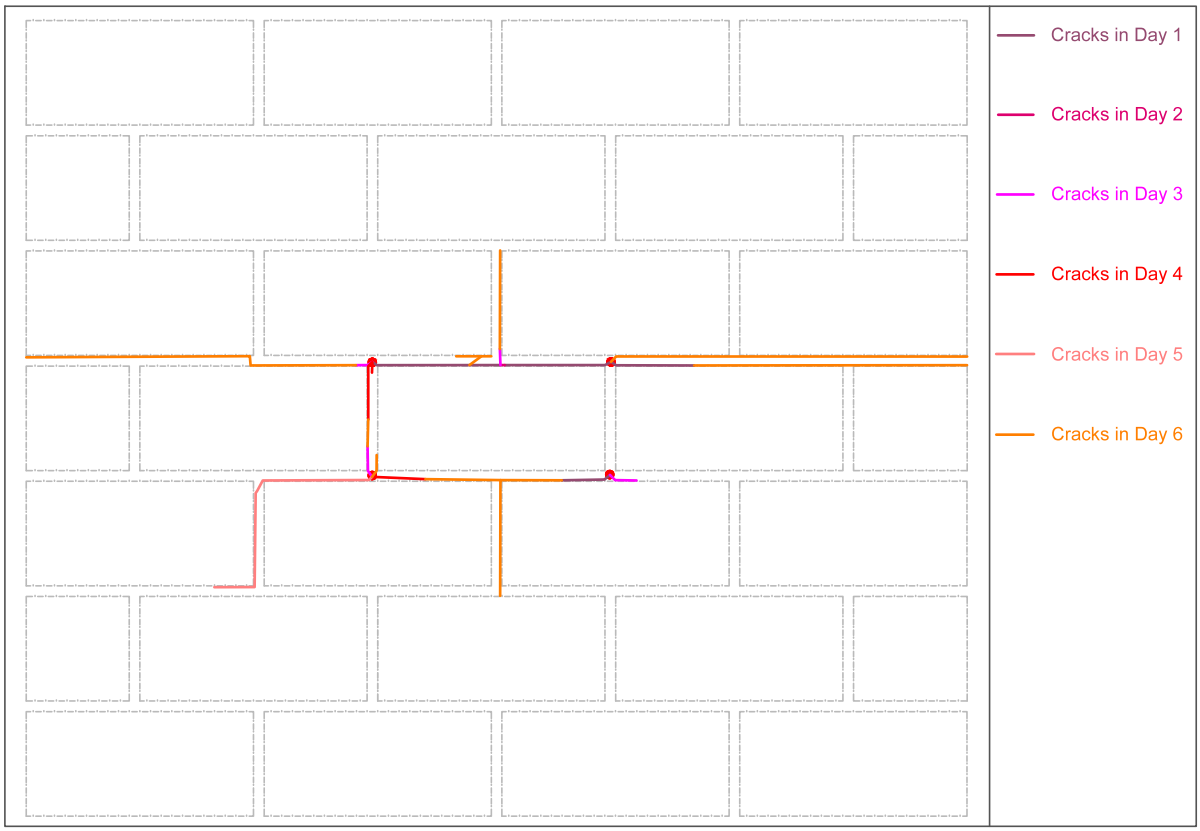

Fig. 18. Wall 4 crack propagation

5.3 Hole Spacing

In terms of hole spacing, Dowding and Labuz (1982) proposed that the volume of demolished material could be optimized using a ratio of hole spacing (S) over hole diameter (D) and recommended an S/D = 16 for dolomite blocks of 165MPa. Applying the recommended ratio to the unit masonry testing herein would result in a spacing of 80mm. The actual minimum spacing was 113mm in the vertical direction (S/D = 22.6), which was 140% larger than Dowding and Labuz's (1982) recommendation. The research herein also had a maximum spacing of 225mm (S/D = 45). BASF Construction Chemicals UK Ltd. (2016) recommends a spacing of 400-600mm with a drill hole diameter of 36-50mm for horizontally oriented, hard rock samples (S/D = 11 to 12) [Fig. 19]. These show a general trend of higher spacing to diameter ratios with weaker surrounding material, but in general all had relatively low S/D values compared to the S/D=45 used herein, which may account for the incomplete cracking.

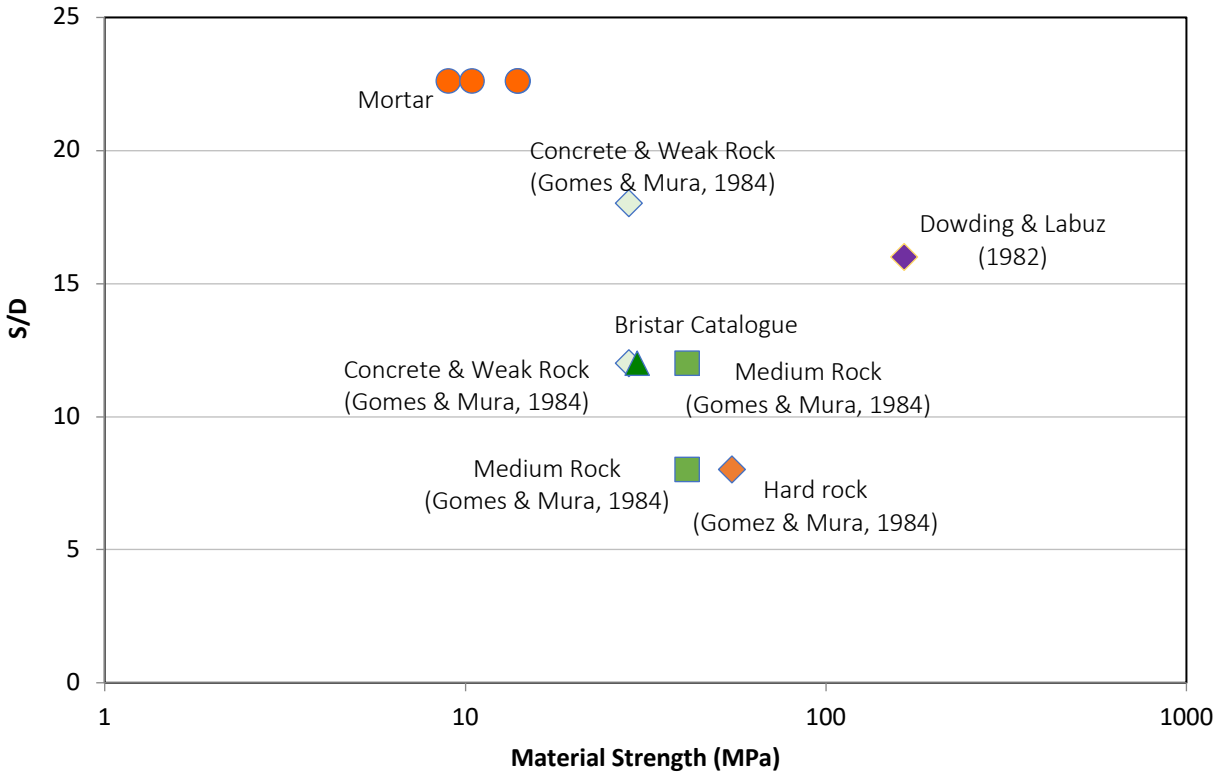

Fig. 19. Proposed relationship between S/D ratio and material strength

Ingraffea and Beech (1982) concluded that if drill-hole spacing was too large, demolition would be incomplete. Therefore, as cracking propagated in almost all holes in the masonry and the partial demolition of the wall was complete, the horizontal spacing of 225mm with 5mm diameter drill holes proved effective for partial masonry unit removal but was not sufficient for the selective removal of an isolated unit, in part due to the extensive confinement of the surrounding masonry. In the testing herein, some unintentional cracks also propagated when hole spacing was closer and the distance to the free edge was smaller. As Tang et al. 2017 noted, once a crack had propagated half of the distance to the edge of the sample, it grew faster than the other cracks and reached the boundary sooner, which was similar to the major versus minor cracks found by Huynh et al. (2017), but in that case the cracks then progressed downward, unlike in the work by Tang et al. (2017), where the cracks stopped propagating and only expanded. Most recently, experimental and numerical results by De Silva and Ranjith (2019) also demonstrated that crack propagation was directly

influenced by the distance to the boundary from SCDA drill hole. In summary, as previous guidelines were designed for concrete and rock demolition, a 225mm spacing should be considered as a starting point for future efforts for unit masonry.

5.4 Hole Diameter Size Effect

With regard to the effect of hole diameter size, Dowding and Labuz (1982) reported that larger drill-hole diameters produced cracks sooner than smaller holes in identical stone samples tested at the same ambient temperature. This was also supported by research by Laefer et al. (2018) which compared 50.8mm, 76.2mm, and 101.6mm diameter pipes in a water bath, in which larger diameter pipes consistently generated greater expansive pressure. This was presumed to be caused by the greater amount of SCDA which produced higher temperatures in accelerated timeframes and more pressure, as opposed to just the diameter size. Specifically, quadrupling the volume of SCDA in the pipe accelerated the heat of hydration by 2°C in the middle of the pipe. Those higher temperatures translated to higher expansive pressures. In that case, a 20% increase in the volume of material resulted in a 700% increase in expansive pressure.

In that testing arrangement, the difference in SCDA quantities was significant, which raises the question of whether a small change in hole diameter could influence the cracking. A comparison of Specimen 2 to the outcomes of comparable materials tested under similar ambient temperatures but with smaller holes (Natanzi et al., 2016b) provides some insight. Specifically, the wallettes by Natanzi et al. (2016b) were 1/6th the size of Specimen 2 with a hole diameter of only 3.97mm (versus 5mm). These specimens also had a TFC of approximately 9 hours. The maximum crack widths were also similar (9.4mm for the 3.97mm hole versus 10.76 mm for the 5mm hole herein). However, the average crack length per hole in the research conducted herein was greater for the larger diameter hole specimens [239.4mm in Natanzi et al. (2016b) versus 418mm for the specimens herein], giving further credence to the concept of the amount of SCDA being a controlling factor.

Cracks tended to occur at the interface between the brick and the mortar, while the masonry units themselves remained intact, as was seen in the work by Natanzi et al. (2016b). Typically, cracking was either horizontal or vertical in orientation, as also reported by Tang et al. (2017) in homogeneous sampes. Some secondary cracks formed radially around the holes but later joined the primary horizontal or vertical cracks. As De Silva (2019) mentioned, the tangential strains and tensile hoop stresses surrounding the borehole facilitates the tensile fracture around the borehole in the direction perpendicular to the axis of the borehole. This aligns with Bristar's Technical Manual (2010), which predicts 2-4 cracks radiating from each filled drill hole. The specimens herein generated between 1 and 3 cracks (Figs. 5-8), while the work by Natanzi et al. (2016b) observed an average of 2 cracks per hole.

6 LIMITATIONS

These experimental tests were conducted with a single-wythe wall, without any additionally applied load. Consequently, SCDA demolition time and crack propagation speed and pattern can be slower under real-world loading if there is additional confinement. As this was a very preliminary study, significant parameters such as wall size and weight, bonding strength, and three-dimensional aspects, all of which are likely to influence the time and pattern of demolition, could not be considered, nor could the need to study the impact on multiple wythe walls. Furthermore, as walls are largely exposed on only one side with insulation on the other, the role of ambient temperature and the diurnal impact of temperature in the field is wholly unexplored.

7 CONCLUSIONS

Four laboratory-based sample unit masonry walls were subjected to selective demolition using SCDA Bristar 150. Each specimen featured a different drill hole layout, mortar type, brick type, and number of drill holes. The drill hole diameter and depth were maintained at 5mm and 70mm, respectively for each sample. The ambient temperature was uncontrolled and ranged between 17-23°C during the 3 weeks of monitoring. This pilot study was intended to provide a preliminary feasibility assessment of the use of SCDAs for selective and partial demolition of unit masonry structures.

Due to lack of confinement, cracks in all specimens initially generated in the upper part of the specimens. Specimens with more drill holes generated more cracks and wider cracks, while the weakest specimen cracked first and exhibited the highest crack propagation speed. Generally, the time to first crack was 9-11 hours for unit masonry with compressive strengths of 8.99–14.02MPa. At the end of testing, an average crack length per hole of 418mm was measured, and an average maximum crack width of 5.22mm was recorded. Hole diameter and spacing proved sufficient for cracking the mortar, but removal was only successful in the specimen with a diagonal hole pattern in two parallel lines; a single diagonal line was not tested. For time-constrained projects, more closely spaced holes could be considered for faster overall demolition, as cracking would be more widespread at an earlier point in time; larger holes were not possible without damaging the masonry units, which may or may not be important depending upon the project. On average, 93% of crack propagation occurred within the first four days and was especially notable within the first two days, with accompanying crack width. Interestingly, cracks continued to expand for up to 3 weeks after insertion of SCDA, even though hydration heat was only apparent in the first 14 days. Though selective removal of a single unit was not achieved, this experimental work demonstrated the viability of using SCDAs for partial demolition of full-scale unit masonry in both weak and relatively strong mortars, as cracking was fully confined to the mortar, with little unintentional additional cracking occurring and no cracking of the masonry units. Having an open face could also facilitate the selective removal of the wall.

ACKNOWLEDGMENTS

The authors would like to thank Mr. Derek Holmes and Mr. John Ryan, lab technicians, University College Dublin for their tireless efforts in the lab throughout the research. This work was funded by Science Foundation Ireland grant 12/ERC/12534.

REFERENCES

Argila, A. (2008). *Device for directing mortar droppings/debris, protecting a drainage weep device and draining water from a single wythe wall, the single wythe wall provided with the device, and method of draining water from the single wythe wall*. U.S. Patent 7,386,956.

Arshadnejad, S., Goshtasbi, K., & Aghazadeh, J. (2011). "A model to determine hole spacing in the rock fracture process by non-explosive expansion material." *International Journal of Minerals, Metallurgy, and Materials*, 18(5), 509-514. doi:10.1007/s12613-011-0470-5

ASTM International (American Society for Testing and Materials). (2014a). "Standard Specification for Mortar for Unit Masonry" *C270-14a*, West Conshohocken, PA.

ASTM International (American Society for Testing and Materials). (2014b). "Standard Test Method for Compressive Strength of Masonry Prisms" *C1314-14*, West Conshohocken, PA.

BASF Construction Chemicals UK Ltd. (2016). "Bristar" <http://www.epmssupplies.co.uk/admin/products/documents/BASF%20(Feb%20-%20MBT)/Health/POWERBRISTARMSDS.pdf> (Mar. 4 2016)

"Bristar Non-Explosive Demolition Agent Technical Manual", (2010), <http://www.taiheiyom.co.jp/archives/002/201104/4dafb63d1df1f.pdf> (Nov. 3, 2014].

De Silva, V. R. S., Ranjith, P. G., Perera, M. S. A., & Wu, B. (2019). The effect of saturation conditions on fracture performance of different soundless cracking demolition agents (SCDAs) in geological reservoir rock formations. *Journal of Natural Gas Science and Engineering*, *62*, 157-170.

De Silva, V. R. S., & Ranjith, P. G. (2019). Evaluation of injection well patterns for optimum fracture network generation host-rock formations: An application in in-situ leaching. *Minerals Engineering*, *137*, 319-333.

Dessouki, A. E., and Mitri, H. (2011). "Rock Breakage Using Expansive Cement." *Engineering,* 3(02), 168-173, 10.4236/eng.2011.32020

Dhanasekar, M., and Xiao, Q. Z. (2001). "Plane hybrid stress element method for 3D hollow bodies of uniform thickness." *Computers & Structures*, 79(5), 483-497.

Dowding, C. H., and Labuz, J. F. (1982). "Fracturing of rock with expansive cement." *Journal of Geotechnical Engineering ASCE,* 109, 1288-1299.

Drysdale, R. G., and Hamid, A. A. (1982). "Anisotropic tensile strength characteristics of brick masonry." *Proc., Sixth Int. Brick-Masonry Conf.,* Associazione Nazionale Industriali Dei Laterizi (ANDIL), Rome, Italy, 143-153.

Gambarotta, L., and Lagomarsino, S. (1997). "Damage Models for the Seismic Response of Brick Masonry Shear Walls. Part I: The Mortar Joint Model and Its Applications." *Earthquake Engineering & Structural Dynamics,* 26(4), 423-439, 10.1002/(SICI)1096-9845(199704)26:4<423:AID-EQE650>3.0.CO;2-#

Gambatese, J. A. (2003). "Controlled concrete demolition using expansive cracking agents." *Journal of Construction Engineering and Management,* 10.1061/(ASCE)0733-9364(2003)129:1(98), 98-104.

Gleeson, W. 2018. https://www.timeout.com/newyork/news/riis-parks-historic-art-deco-bathhouse-is-getting-a-major-upgrade-062718.

Gomez, C., and Mura, T. (1984). "Stresses caused by expansive cement in hole." *J. Engineering Mechanics,* 110(6), 1001-1005.

Goto, K., Kojima, K., and Watabe, K. (1988). "The mechanism of expansive pressure and blow-out of static demolition agent." Paper presented at the *Second International RILEM Symposium on Demolition and Reuse of Concrete and Masonry*, Tokyo, Japan.

Harada, T., Idemitsu, T., & Watanabe, A. (1985). "Demolition of Concrete with Expansive Demolition Agent." *Proceedings of the Japan Society of Civil Engineers,* 360, 61-70.

Harada, T., Idemitsu, T., Watanabe, A., and Takayama, S.-I. (1989). The Design Method for the Demolition of Concrete with Expansive Demolition Agents. In S. Shah & S. Swartz (Eds.), *Fracture of Concrete and Rock* (pp. 47-57), Springer, New York.

Hinze, J., and Brown, J. (1994). "Properties of soundless chemical demolition agents." *Journal of Construction Engineering and Management ASCE,* 10.1061/(ASCE)0733-9364(1994)120:4(816), 816-827.

Huynh, M.-P., Laefer, D., McGuill, J., White, A. (2017). "Temperature-related Performance Factors for Chemical Demolition Agents" Int'l J. Masonry Res. & Innov., Inderscience. Vol. 2, Nos. 2/3, 220-240, http://dx.doi.org/10.1504/IJMRI.2017.10006805

Huynh, M. P., and Laefer, D. (2009). "Expansive cement and soundless chemical demolition agents: state of technology review." Paper presented at the *11th Conference on Science and Technology*, Ho Chi Minh City, Vietnam.

Ingraffea, A. R., & Beech, J. F. (1982). "Fracturing of rock with expansive cement." *Journal of Geotechnical Engineering ASCE,* 109, 1205-1208.

Laefer, D. F. (2001). *Prediction and assessment of ground movement and building damage induced by adjacent excavation*. Phd dissertation, University of Illinois at Urbana-Champaign, Urbana, IL.

Laefer, D., Elliott, A. and Weller, L., 2002. The temporary use of drilled shafts in the renovation of Carnegie Hall. Deep Foundations 2002: An International Perspective on Theory, Design, Construction, and Performance pp. 320-334.

Laefer, D. F., Boggs, J., and Cooper, N. (2004). "Engineering Properties of Historic Brick: Variability Considerations as a Function of Stationary versus Nonstationary Kiln Types." *Journal of the American Institute for Conservation*, 43(3), 255-272.

Laefer, D.F, Cooper, N., Minh, P., Midgette, J., Wortman, J., and Ceribasi, S. (2010). "Behavioral Aspects of an Expansive Fracture Agent during Cracking of Unreinforced Concrete." *Mag. Concrete Research*, 62(6), 443-452, 10.1680/macr.2010.62.00.1.

Laefer, D. F., Natanzi, A. S., & Zolanvari, S. I. (2018). "Impact of thermal transfer on hydration heat of a Soundless Chemical Demolition Agent." *Construction and Building Materials*, *187*, 348-359, https://doi.org/10.1016/j.conbuildmat.2018.07.168

Natanzi, A. S., and Laefer, D. F. (2014). *Using chemicals as demolition agents near historic structures*. Paper presented at the 9th International Conference on Structural Analysis of Historical Constructions, Mexico City, Mexico.

Natanzi, A. S., Laefer, D. F., and Connolly, L. (2016a). "Cold and moderate ambient temperatures effects on expansive pressure development in soundless chemical demolition agents." *Construction and Building Materials,* 110, 117-127, 10.1016/j.conbuildmat.2016.02.016

Natanzi, A. S., Laefer, D. F., and Mullane, S. (2016b). "Chemical demolition of unit masonry: A preparatory study." *Proc., Structural Analysis of Historical Constructions–Anamnesis, diagnosis, therapy, controls*, CRC Press, Boca Raton, FL, 88-95.

Pavia, S., Fitzgerald, B., and Treacy, E. (2006). "An assessment of lime mortars for masonry repair." *Proc., Concrete Research in Ireland Colloquium,* C. McNally, ed., University College Dublin, Dublin, Ireland, 101-108.

Senthivel, R., and Lourenço, P. B. (2009). Finite element modelling of deformation characteristics of historical stone masonry shear walls. *Engineering Structures,* 31(9), 1930-1943, 10.1016/j.engstruct.2009.02.046.

Tang, S. B., Huang, R. Q., Wang, S. Y., Bao, C. Y., & Tang, C. A. (2017). Study of the fracture process in heterogeneous materials around boreholes filled with expansion cement. *International Journal of Solids and Structures*, *112*, 1-15.